Aus der Medizinische Klinik mit Schwerpunkt Kardiologie
der Medizinischen Fakultät Charité – Universitätsmedizin Berlin

DISSERTATION

Impact of mesenchymal stromal cells on streptozotocin-induced diabetic cardiomyopathy

zur Erlangung des akademischen Grades
Doctor medicinae (Dr. med.)

vorgelegt der Medizinischen Fakultät
Charité – Universitätsmedizin Berlin

von
Gang Huang
aus Sichuan, Volksrepublik China

Datum der Promotion: 01.03.2019

CONTENTS

ZUSAMMENFASSUNG **V**

ABSTRACT **VII**

ABBREVIATIONS **IX**

1. INTRODUCTION **1**

1.1 Diabetes mellitus 1

1.2 Diabetic cardiomyopathy 1

1.2.1 Cardiac structural changes 2

1.2.2 Cardiac functional changes 2

1.2.3 Potential mechanism 3

1.3 Animal models of diabetes mellitus 3

1.3.1 Animal models of type 1 diabetes mellitus 3

1.3.2 Animal models of type 2 diabetes mellitus 6

1.4 Treatment 7

1.4.1 Traditional treatment 7

1.4.2 Cell-based therapy 7

1.4.2.1 Stem cells 7

1.4.2.2 Adult stem cells 8

1.4.2.3 Mesenchymal stromal cells 8

2. RATIONALE **11**

3. MATERIALS AND METHODS **12**

3.1 Materials and equipment 12

3.1.1 Materials 12

3.1.2 Equipment 13

3.1.3 Buffer and reagent 13

3.1.4 Primers 15

3.1.5 Antibodies 15

3.1.6 Software 16

3.2 Methods 17

3.2.1 Study design 17

3.2.2 Streptozotocin-induced diabetes model establishment 17

3.2.2.1 Mouse strains and animal care 17

3.2.2.2 Streptozotocin preparation 17
3.2.2.3 Streptozotocin injection 17
3.2.2.4 Blood glucose monitoring and HbA1c measurement 19
3.2.3 Bone marrow-derived mesenchymal stromal cell intervention 19
3.2.4 Catheter–based hemodynamic measurements 19
3.2.4.1 Measurement Procedure 19
3.2.4.2 Tissue collection 21
3.2.5 Immunohistochemical analysis 21
3.2.5.1 Cryosections 21
3.2.5.2 Immunohistochemical staining 21
3.2.5.3 Digital image analysis 22
3.2.6 Gene expression analysis 23
3.2.6.1 RNA extraction 23
3.2.6.2 Reverse Transcription 23
3.2.6.3 Real-time polymerase chain reaction 24
3.2.6.4 Housekeeping gene 24
3.2.7 Flow cytometry analysis 25
3.2.7.1 Immunomodulatory effects of MSCs 25
3.2.7.2 Splenic regulatory T cells 26
3.2.7.3 Splenic cytokine production 26
3.2.7.4 Splenocyte activation and proliferation 27
3.3 Statistical analysis 28
4. RESULTS 29
4.1 Blood glucose and HbA1c levels 29
4.2 Cardiac function parameters 31
4.3 Left ventricle fibrosis 33
4.3.1 Gene expression 33
4.3.2 Immunohistological evidence 35
4.3.2.1 Extracellular matrix protein collagen I expression 35
4.3.2.2 Extracellular matrix protein collagen III expression 36
4.3.2.3 Alpha-smooth muscle actin protein expression 37
4.4 Left ventricle inflammation 37
4.4.1 Gene expression 37
4.4.2 Immunohistological evidence 40

4.4.2.1 CD4+ T lymphocytes 40
4.4.2.2 CD8a+ cytotoxic T lymphocytes 41
4.4.2.3 CD68+ monocytes/macrophages 42
4.5 Immune regulation of splenocytes 43
4.6 The pro-fibrotic potential of splenocytes 46
5. DISCUSSION 47
5.1 Main findings 47
5.2 Impact of BM-MSCs on blood glucose and HbA1c in streptozotocin-induced diabetic mice 47
5.3 Impact of BM-MSCs on cardiac function in streptozotocin-induced diabetic mice 48
5.4 Impact of BM-MSCs on cardiac fibrosis in streptozotocin-induced diabetic mice 49
5.5 Impact of BM-MSCs on immune cell infiltration and splenic immune cell activities in streptozotocin-induced diabetic mice 49
6. PERSPECTIVES 52
BIBLIOGRAPHY 53
EIDESSTATTLICHE VERSICHERUNG 69
CURRICULUM VITAE 70
PUBLIKATIONSLISTE UND KONGRESSBEITRÄGE 71
ACKNOWLEDGEMENTS 72

ZUSAMMENFASSUNG

Hintergrund: Mesenchymale stromale Zellen (MSZ) haben kardial regenerative, antifibrotische und entzündungshemmende Eigenschaften und wurden zur Behandlung des Diabetes Mellitus (DM) und der experimentellen diabetischen Kardiomyopathie mit vielversprechenden Ergebnissen eingesetzt. Jedoch wurde der Einfluss von $CD362^+$-selektierten MSZ bei der experimentellen diabetischen Kardiomyopathie bisher noch nicht untersucht. Ziel dieser Studie war es daher, die potenzielle Wirkung von $CD362^+$-MSZ gegenüber von $CD362^-$-MSZ und Wildtyp (WT)-MSZ auf die diabetische Kardiomyopathie, im Modell des Streptozotocin (STZ)-induzierten Typ 1 DM, zu untersuchen.

Methoden: C57BL6/J Mäuse (Charles River, männlich, 8 Wochen) wurden randomisiert den Kontroll-, STZ-, STZ WT-, STZ $CD362^-$ und STZ $CD362^+$ Gruppen zugeordnet. Durch die Gabe von STZ (50mg/kg) an 5 aufeinanderfolgenden Tagen wurde der DM in den Tieren induziert. Vier Wochen nach der STZ-Applikation wurden jeweils $1x10^6$ Knochenmarks-abgeleitete $CD362^+$-MSZ, $CD362^-$-MSZ oder WT-MSZ intravenös in den drei Interventionsgruppen verabreicht. Vier Wochen nach der Intervention wurden die Mäuse einer hämodynamischen Messung unterzogen und anschließend geopfert. Es wurden Blut und Organe zur Bestimmung der Blutglukose (BG) und dem glykosylierten Hämoglobin A1c (HbA1c), sowie für immunhistologische Untersuchungen und Genexpressionsanalysen entnommen.

Ergebnisse: Vier Wochen nach MSZ-Applikation waren weder die BG- und die HbA1c-Spiegel, noch die dysregulierte LV-Funktion in den behandelten STZ-Mäusen positiv beeinflusst. Es handelte sich hierbei um ein Modell mit gering ausgeprägter Entzündung, charakterisiert durch eine unveränderte kardiale VCAM-1, TNF-α und IL-1ß Genexpression und einer gleichbleibenden Anzahl an $CD68^+$, $CD4^+$ und $CD8^+$ Zellen im Herzen. Im Gegensatz dazu, waren die TGF-ß, ICAM-1 und S100A9 mRNA-Expression um das 1,4-fache ($p < 0,01$), 1,4-fache ($p < 0,05$) bzw. 2,6-fache ($p < 0,05$) im LV erhört, wohingegen keine Myokardfibrose induzierte wurde. Keine der drei MSZ-Typen verringerte die gesteigerte TGF-ß, ICAM-1 und S100A9 Expression. Des Weiteren, konnte eine 2,2-fach ($p < 0,05$) höhere Anzahl an TGF-ß-exprimierende $CD68^+$ Zellen in der Milz von STZ-Tieren gegenüber den Kontrollmäusen detektiert

werden, was mit einem 1,5-fach ($p < 0,05$) höherem profibrotischem Potential assoziiert war. WT-MSZ und $CD362^+$-MSZ verringerten die Zahl an TGF-ß-exprimierende $CD68^+$ Zellen um das 6,0-fache ($p=0,0001$) bzw. 4,5-fache ($p<0,001$), was sich jedoch nicht in einer Reduktion des profibrotischem Potentials der Splenozyten aus STZ-Mäusen wiederspiegelte.

Schlussfolgerung: In diesem Modell mit gering gradiger Entzündung, keiner ausgeprägten Myokardfibrose und keiner kompensatorischen Herzfunktionsstörung, verringert keiner der applizierten MSZ die BG und HbA1c-Spiegel, das profibrotische Potenzial der Splenozyten oder die Herzfunktion. Jedoch reduzierten WT-MSZ $CD362^+$-MSZ den prozentualen Anteil an TGF-ß-exprimierende $CD68^+$ Zellen in der Milz.

ABSTRACT

Background: Mesenchymal stromal cells (MSCs) have cardiac regenerative, anti-fibrotic, and anti-inflammatory properties and have been used for the treatment of diabetes mellitus (DM) and experimental diabetic cardiomyopathy with promising results. The impact of $CD362^+$ selected MSCs on experimental diabetic cardiomyopathy has not been studied before. Therefore, this study was aimed to explore the potential impact of $CD362^+$ versus $CD362^-$ and wild type (WT) MSCs on diabetic cardiomyopathy in a streptozotocin (STZ)-induced type 1 DM mouse model.

Methods: C57BL/6J mice (Charles River, male, 8-week-old mice) were randomly assigned to control, STZ, STZ WT, STZ $CD362^-$ and STZ $CD362^+$ groups. DM was induced via STZ administration (50 mg/kg) for consecutive 5 days. Four weeks after STZ administration, $1x10^6$ bone marrow-derived $CD362^+$, $CD362^-$ and WT MSCs were intravenously administered in the three intervention groups. Four weeks after MSCs administration, mice were hemodynamically characterized before sacrifice and organs were harvested for subsequent blood glucose (BG), glycated hemoglobin A1c ($HbA1_c$), immunohistological and gene expression analysis.

Results: Four weeks after MSCs application, none of the MSCs decreased BG or $HbA1_c$ levels in STZ mice, nor did they alter the dysregulated LV function. In this model of low-level inflammation with unchanged LV vascular cell adhesion molecule 1, TNF-α, IL-1ß mRNA expression and unaltered CD68, CD4 and CD8 presence, LV TGF-ß, ICAM-1 and S100A9 mRNA expression was increased 1.4-fold ($p<0.01$), 1.4-fold ($p<0.05$), and 2.6-fold ($p<0.05$), respectively, whereas cardiac fibrosis was not induced. None of the MSCs decreased the upregulated TGF-ß, ICAM-1 or S100A9 expression. Splenic TGF-ß-expressing CD68 cells were 2.2-fold ($p<0.05$), higher in STZ versus control mice, which was translated into a 1.5-fold ($p<0.05$) higher pro-fibrotic potential. WT MSCs and $CD362^+$ cells decreased TGF-ß-expressing CD68 cells by 6.0-fold ($p=0.0001$) and 4.5-fold ($p<0.001$), respectively, but none of the MSCs decreased the profibrotic potential of the splenocytes in STZ mice.

Conclusions: In this model of low-level inflammation, no pronounced cardiac fibrosis and compensatory cardiac dysfunction, none of the MSCs decreased BG, $HbA1_c$ levels,

the profibrotic potential of splenocytes and altered cardiac function, whereas WT MSCs and $CD362^+$ cells reduced the percentage of TGF-ß-expressing CD68 cells.

ABBREVIATIONS

ABC	avidin-biotin complex
ANOVA	analysis of variance
AF	area fraction
α-SMA	alpha-smooth muscle actin
BM	bone marrow
BG	blood glucose
Ca^{2+}	calcium
CD	cluster of differentiation
cDNA	complementary DNA
CHD	coronary heart disease
DM	diabetes mellitus
DNA	deoxyribonucleic acid
dP/dt_{max}	maximum left ventricular pressure rise rate
dP/dt_{min}	maximum left ventricular pressure drop rate
EDTA	ethylenediaminetetraacetate
EF	ejection fraction
FOXP3	transcription factor forkhead box protein P3
$HbA1_c$	glycated hemoglobin A1c
HF	heart failure
HFrEF	ejection fraction reduced heart failure
IHC	immunohistochemistry
IL	interleukin
i.p.	intraperitoneal
i.v.	intravenous
LV	left ventricular / left ventricle
LVESV	the volume of the LV at the end of systole
LVEDV	the volume of the LV at the end of diastole
LVESP	the pressure in the LV at the end of systole
LVEDP	the pressure in the LV at the end of diastole
mRNA	message RNA

MNC	mononuclear cell
MSC	mesenchymal stromal cells
PBS	phosphate-buffered saline
PCR	polymerase chain reaction
PV	pressure-volume
REDDSTAR	Repair of Diabetic Damage by Stromal Cell Administration
RNA	ribonucleic acid
RT	room temperature
SEM	standard error of the mean
STZ	streptozotocin
SV	Stroke volume
TGF-β	transforminutes g growth factor-beta
TNF-α	tumor necrosis factor-alpha
Tregs	regulatory T cells

1. INTRODUCTION

1.1 Diabetes mellitus

Diabetes mellitus (DM) is a life-long chronic disease, characterized by relative or absolute insulin deficiency caused by pancreatic β-cell dysfunction and insulin resistance in target organs. Type 1 DM is characterized by absolute insulin deficiency and type 2 DM by relative insulin deficiency. Type 1 DM is considered as an autoimmune disease with a progressing decline of insulin levels. According to data from the World Health Organisation, there were 422 million people aged over 18 years who suffered from DM globally in 2014. The number of DM has steadily risen over the past few decades. The prevalence among adults has substantially increased from 4.7% in 1980 to 8.5% in 2014 worldwide, and 1.5 million deaths were worldwide directly caused by DM in 2012 [1]. In Europe, the incidence of type 1 DM increases by about 3.9% annually [2]. The most common complications of DM are microvascular and macrovascular complications, including coronary heart diseases (CHD), stroke, and renal dysfunction. Type 2 DM was the sixth leading cause of disability in 2015. Cardiovascular diseases are the greatest cause of morbidity and mortality associated with type 2 DM and needs intensive management of glucose and lipid concentrations as well as blood pressure to minimize the risk of complications and disease progression [3]. Compared to non-diabetes, type 2 DM patients have a 15% higher risk of all cause death [4]. A meta-analysis, covering nearly seventy-thousand people demonstrated that patients with DM had an increased risk of CHD, ischemic stroke, and other deaths related to vascular disease [5].

1.2 Diabetic cardiomyopathy

Diabetic cardiomyopathy was first described by Rubler *et al.* [6] and refers to abnormal changes in myocardial function or cardiac structure in the absence of coronary artery disease, hypertension and valvular diseases. The worst outcome of diabetic cardiomyopathy is heart failure (HF). About 40% of HF patients with reduced ejection fraction (EF) (HFrEF) have DM and hospitalized DM patients are associated with a worse prognosis compared to non-diabetic patients [7]. A retrospective study reported that in diabetic patients, the incidence of chronic HF was 2.5 times higher compared to that non-diabetic patients [8].

The pathogenesis of diabetic cardiomyopathy is likely to be a multifactorial process. Insulin resistance and hyperglycemia are main factors in the pathophysiological progression of cardiomyopathy, which cause complex cellular and molecular changes that predispose to altered myocardial structure and function [9].

1.2.1 Cardiac structural changes

Interstitial and perivascular fibrosis, intramyocardial microangiopathy, interstitial inflammation, cardiac apoptosis, abnormal intracellular calcium (Ca^{2+})-handling, endothelial dysfunction, a defect in substrate metabolism and cardiac hypertrophy are characteristics of diabetic cardiomyopathy [10]. Left ventricle (LV) hypertrophy is predominant in diabetic cardiomyopathy. In the Framingham Heart study, diabetic women had 10% greater LV mass than non-diabetic patients [11]. An increase in LV mass accompanied by LV thickness is observed in both men and women who suffered from DM [12]. Cardiomyocyte hypertrophy is considered as an effect of hyperglycemia and insulin, which has been verified in animal models [13, 14].

Histopathological changes of diabetic cardiomyopathy include interstitial and perivascular fibrosis in myocardial tissue [6] and increased deposition of intra-myocyte lipids. Interstitial fibrosis in patients with diabetic cardiomyopathy is usually accompanied by cardiomyocyte hypertrophy and microvascular abnormalities, such as thickening of the capillary basement membrane [15]. Myocardial fibrosis in diabetic cardiomyopathy is associated with increased deposition of both type I and III collagen and involves both ventricles [16].

1.2.2 Cardiac functional changes

Progressive diastolic and systolic dysfunctions are major characteristics of diabetic cardiomyopathy. Diastolic dysfunction is determined by a delayed and extended diastolic phase, with impaired early diastolic filling, prolongation of isovolumetric relaxation, increased atrial filling and increased myocardial stiffness, predominantly in the late diastole [17, 18]. Diastolic dysfunction of the LV has been observed in diabetic patients without clinical diabetic cardiomyopathy [19-21] with a prevalence from 40% to 75% by echo measurement [22, 23]. Moreover, diastolic dysfunction is more common than systolic dysfunction in DM [24]. LV diastolic dysfunction in diabetic cardiomyopathy can also gradually progress to systolic dysfunction and may result in LV systolic

dysfunction with reduced LVEF in years [25]. Systolic dysfunction is characterized by the disability of the LV to sufficiently pump blood with oxygen to the body.

1.2.3 Potential mechanism

In the multifactorial pathogenesis of diabetic cardiomyopathy, hyperglycemia, hyperinsulinemia, dyslipidemia and advanced glycation end products trigger cellular signaling, leading to specific alterations in the heart. In type 1 DM, hyperglycemia is the main trigger of cardiac alterations, while in type 2 DM, mainly dyslipidemia plays a major role in the development of diabetic cardiomyopathy [25].

1.3 Animal models of diabetes mellitus

1.3.1 Animal models of type 1 diabetes mellitus

The predominant characteristic of DM type 1 is the autoimmune damage of pancreatic β cells, resulting in insulin deficiency. According to the mechanisms of insulin deficiency induction, there are several rodent models of type 1 diabetes, including chemically-induced, spontaneous autoimmune, genetically-induced, and virally-induced models. (**Table 1** [26])

Table 1. Type 1 Diabetes models for rodent

Induction mechanism	Model	Main features
Chemically Induced	High dose streptozotocin	Simple model of hyperglycaemia
	Alloxan	Model of induced insulitis
	Multiple low dose streptozotocin	
Spontaneous autoimmune	NOD mice	β cell destruction due to an autoimmune process
	BB rats	
	LEW.1AR1/-iddm rats	
Genetically induced	AKITA mice	β cell destruction due to ER stress. Insulin dependent.
Virally-induced	Coxsackie B virus	β cell destruction induced by viral infection of B cells
	Encephalomyocarditis virus	
	Kilham Rat Virus	
	Lymphocytic choriomeningitis virus under insulin promoter	

In chemically-induced type 1 DM models, a high percentage of the endogenous β cells is destroyed, and therefore there is little endogenous insulin production, leading to hyperglycemia. Diabetes is usually induced around 5-7 days prior to the start of the experiment to ensure stable hyperglycemia. Two main compounds used in chemical-induced diabetes models are streptozotocin (STZ) and alloxan.

1.3.1.1 Streptozotocin-induced diabetes model

STZ (2-deoxy-2-({[methyl(nitroso)aminutes o]carbonyl}aminutes o)-β-D-glucopyranose) was first isolated from the soil microorganism *Streptomyces acromogenes* [27]. It has been widely used for the induction of diabetes in experimental animals and in preclinical studies. Among several available chemicals used to induce diabetes, STZ is mostly preferred to model human diabetes in animals, because it has a structure similar to glucose (**Figure 1**) and it enters β cells in a similar way as glucose [28]. STZ-induced diabetes is characterized by profound hyperglycaemia, modest hypertriglyceridaemia, ketosis, and markedly reduced plasma insulin levels. As such, the model is particularly useful in examining the effects of hyperglycaemia in the absence of hyperinsulinaemia. Structural, functional and biochemical alterations observed in STZ-induced diabetes resemble or are comparable to those in human diabetes [29]. STZ-induced diabetes models have been extensively used to investigate the complications of type 1 DM. In mouse models, after administration, STZ enters the pancreatic β cell through the Glut-2 transporter and causes alkylation of the deoxyribonucleic acid (DNA), induces β cell toxicity and death, and triggers a T cell-mediated immune response, similar to human insulin-dependent diabetes [30]. In both mice and rats, depending on the dose, STZ-induced diabetes is associated with interstitial myocardial fibrosis, accompanied by cardiomyocyte hypertrophy, induction of pro-fibrotic and hypertrophy-associated genes, and microvascular rarefaction [31, 32]. STZ is usually administrated as a single high dose (100 to 200 mg/kg) or multiple low doses (20 to 40 mg/kg per day). The dose range depends on the species and strain. Single high-dose administration destroys β cells and produces hyperglycemia rapidly. Multiple low dose-administration induces insulitis in mice and the development of diabetes is dependent on cytokine production. After STZ administration, there is an initial hyperglycemic phase with decreased insulin levels, a second hypoglycemic phase due to a massive release of insulin from ruptured

β cells, and finally a steady hyperglycemic phase involving a rise in blood glucose levels up to 350-400 mg/dL (**Figure 2**)[28].

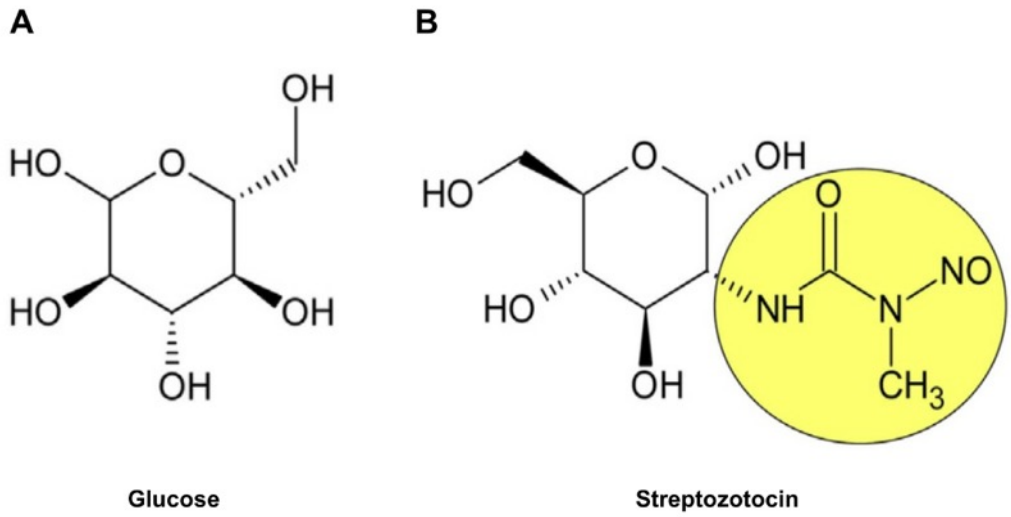

Figure 1. Chemical structures of glucose and streptozotocin [28]**.**

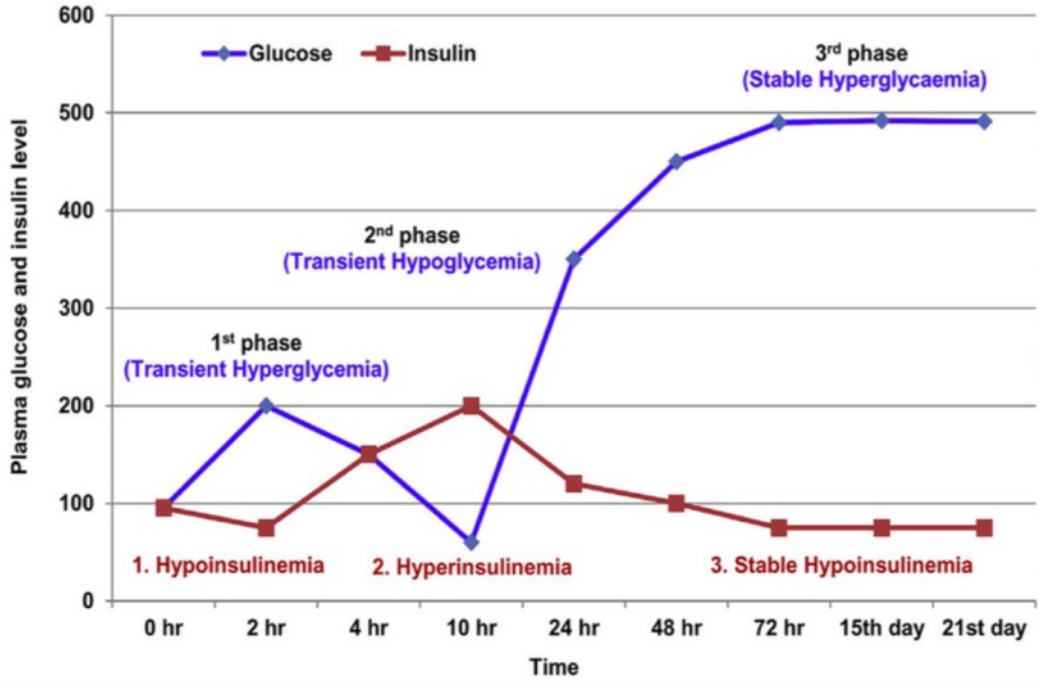

Figure 2. Changes of blood glucose and insulin levels post streptozotocin injection [28]**.**

1.3.1.2 Alloxan-induced diabetes model

Alloxan (2,4,5,6-tetraoxypyrimidine; 5,6-dioxyuracil) is a hydrophilic unstable compound with a structure similar to glucose. These alloxan properties are essential for the

development of diabetes. It induces diabetes mainly by the formation of free radicals after rapid uptake of alloxan by the β cells [33] and oxidation of essential-SH groups and disturbances in intracellular Ca^{2+} homeostasis [34]. Doses in mice range from 50 to 200 mg/kg and in rats from 40 to 200 mg/kg, depending on the strain and the route of administration. Moreover, alloxan has a narrow diabetogenic dose, and a slight overdose could cause general toxicity, especially to the kidney [35].

1.3.2 Animal models of type 2 diabetes mellitus

Insulin resistance and the inability of the β cell to sufficiently produce insulin are the main characteristics of type 2 DM. Therefore, most animal models of type 2 DM are models of insulin resistance and/or models of β cell failure (**Table 2**) [26]. Two commonly used models are the db/db and leptin ob/ob mice. Db/db mice express no leptin receptor and are resistant to the central effects of leptin and develop severe obesity at the age of 1 to 2 months, associated with overt diabetes, hyperinsulinemia and hyperglycemia. Both histochemical staining techniques and biochemical assays have consistently found cardiac fibrosis in db/db mice at the age of 4 to 6 months [36], accompanied by cardiomyocyte hypertrophy and diastolic dysfunction [37]. The most commonly used background is the C57BLKS/J, and they develop ketosis after a few months of age and have a relative short survival period. In 1949, a spontaneous mutation of Leptin in an outbred colony was discovered at the Jackson Laboratory. C57BL/6 mice bred into leptin mutation are the leptin ob/ob mice. Those mice develop obesity, hyperinsulinaemia and hyperglycaemia early. Blood glucose (BG) peaks at 3 to 5 months, after which it falls as the mouse gets older [38]. Other models of type 2 DM are outlined in **Table 2** [26].

Table 2. Type 2 Diabetes models for rodent

Induction mechanism	Model	Main features
Obese models (monogenic)	$Lep_{ob/ob}$ mice	Obesity-induced hyperglycaemia
	$Lepr_{db/db}$ mice	
	ZDF Rats	
Obese models (polygenic)	KK mice	Obesity-induced hyperglycaemia
	OLETF rat	
	NZO mice	
	TallyHo/Jng mice	

	NoncNZO10/LtJ mice	
Induced obesity	High fat feeding (mice or rats)	Obesity-induced hyperglycaemia
	Desert gerbil	
	Nile grass rat	
Non-obese models	GK rat	Hyperglycaemia induced by insufficient β cell function/mass
Genetically induced models of β cell dysfunction	hIAPP mice	Amyloid deposition in islets
	AKITA mice	β cell destruction due to ER stress

1.4 Treatment

1.4.1 Traditional treatment

Generally, DM treatment includes insulin supplementation, diet control, exercise and non-insulin medications [39]. The aim of the treatment is to control glucose level, decrease complications and improve life quality. Currently, treatment of diabetic cardiomyopathy is based mostly on DM treatment combined with HF treatment, including angiotensin-converting enzyme inhibitors, angiotensin II receptor blocker, β-blockers, aldosterone antagonists, and resynchronization therapy [40], while most of these treatment measures have not been fully assessed in diabetic cardiomyopathy patients.

1.4.2 Cell-based therapy

Cell-based therapies or stem cell-based therapies have a huge potential to treat cardiovascular diseases because of their regenerative properties and safety. Until 2013, approximately 2,000 patients have been enrolled in clinical trials around the world to evaluate different kinds of stem cell therapies showing promising results [41].

1.4.2.1 Stem cells

Stem cells are a group of cells, which have the potential capacity to differentiate to different tissue and adult organs, regenerate throughout life and self renew [42]. Stem cells can be broadly categorized into adult stem cells or embryonic/pluripotent stem cells. Stem cell therapy has been investigated in preclinical regenerative studies, including adult stem cells [10] and pluripotent stem cells [43]. Main stem cells already used in cardiac regeneration and repair are listed in **Table3** [44].

Table 3. Stem cells in cardiac regeneration and repair

Type	Source	Advantages	Disadvantages
Embryonic stem cells	Inner cell mass of preimplantation blastocyst	Pluripotent, self-renewal capacity	Graft versus host disease, ethical debate, and tumorgenesis
Mesenchymal stromal cells	Bone marrow, adipose tissue	Multipotent, easy to isolate and expand, lack of immunogenicity	Heterogeneity
Endothelial progenitor cells	Bone marrow, peripheral blood	Movement from bone marrow or peripheral blood, important in neovascularization	Need for expansion, Heterogeneity
Skeletal Myoblasts	Skeletal muscle	High scalability, resistance to ischemia, multipotent, no teratoma formation	Electrophysiologically incompatible, lack of gap junction
Cardiac stem cells	Heart	Resident cells, robust cardiovascular differentiation potential, reduced tumor formation	short survival, and limited supply

1.4.2.2 Adult stem cells

Adult stem cells are multipotent cells that have been identified in many fully developed organs. These include populations from extra-cardiac sources (bone marrow(BM)-derived mononuclear cells, BM-derived mesenchymal stem cells, adipose-derived mesenchymal stem cells and endothelial progenitor cells). Adult stem cells are considered multi-potent and have some limited ability to form various differentiated cell types. *In vitro*, adult stem cells can differentiate into multiple cell types, including cardiomyocytes. Adult stem cells have shown encouraging results of repair of the injured heart [41] mostly through paracrine actions [45], and modulation of the extracellular matrix [46].

1.4.2.3 Mesenchymal stromal cells

1.4.2.3.1 Characteristics

Mesenchymal stromal cells (MSCs) are multipotent stem cells and comprise a heterogeneous population of cells. MSCs have been first isolated from BM [47], where MSCs represent a rare population and are 10-fold less abundant than hematopoietic stem cells [48]. MSCs can be easily grown and expanded in culture. In 2006, the International Society for Cellular Therapy unified the minimal criteria of MSCs. MSCs should 1) adhere to plastic in standard culture conditions, 2) express CD105, CD90, CD73, and CD44, without expression of CD45, CD34, CD14 or CD11b, CD79 or CD19 and human leukocyte antigen-DR; 3) be able to differentiate into osteoblasts,

adipocytes and chondroblasts *in vitro* [49]. Markers to sort MSCs such as STRO-1 [50], antinerve growth factor receptor CD271 [51], or cell adhesion molecule CD146 [52], transforming growth factor-β (TGF-β) receptor complex CD105 [53], cell surface protein CD106 [54], membrane glycoprotein CD146 [55], cell surface tyrosine kinase receptor CD140a [56] and CD140b [57], intermediate filament protein nestin [58], and alpha-chemokine receptor CXCR-4 [59] describe the heterogeneity and clonogenic capacity of these cells. By either local or systemic route administration, the myocardial homing capacity of MSCs is weak [60-62]. However, MSCs are attracted to the injured organs through a chemotaxis process in which MSCs recognize over-expressed molecules (stromal cell-derived factor-1, monocyte chemoattractant protein-1, and chemokine receptor type 2 surface receptors etc.) in injured tissues [63], resulting in a selective homing after systemic administration. MSCs are considered as hypoimmunogenic cells, since they are not rejected by the recipient's immune system, even if they come from non-histocompatible individuals [64], that because they lack expression of major histocompatibility II [65] and the costimulatory molecules CD80, CD86 or CD40 [66]. Thus, MSCs will not lead to proliferation of allogeneic and autoreactive lymphocytes, which is an important advantage for allogeneic transplantation therapies.

1.4.2.3.2 Cardiac effects of mesenchymal stromal cells

MSCs are self-renewal cells with the possibility to differentiate into other kind of cells. It has been demonstrated that MSCs are able to differentiate into cardiomyocytes, endothelial cells, and smooth muscle cells [67]. Moreover, MSCs can express specific cardiomyocyte markers (for example, connexin 43 and N-cadherin) [68, 69]. MSCs secrete paracrine factors involved in regenerative and cardiac remodeling, such as insulin-like growth factor, hepatocyte growth factor, endothelin-1, basic fibroblast growth factor (with proliferative and anti-apoptotic properties), vascular endothelial growth factor and platelet-derived growth factor (with angiogenic properties), and matrix metallopeptidase-9 [70, 71]. Also, MSCs have anti-inflammatory properties through the activation, suppression, migration, or differentiation of specific immune system cells, including B cells, T cells, natural killer cells, macrophages, dendritic cells, and neutrophils, by the secretion of several immune regulators, including TGF-β, IL-4, IL-6, IL-10, PGE2, and indoleamine 2,3-dioxygenase [72]. Moreover, MSCs decrease elevated tissue oxidative stress by modifying the redox microenvironment and reduce

reactive oxygen species-induced apoptosis [73]. Besides these anti-inflammatory, anti-oxidative, anti-fibrotic, anti-apoptotic, and pro-angiogenic effects. MSCs activate cardiac progenitor cell proliferation and differentiation [74].

1.4.2.3.3 CD362 and CD362^{+} selected mesenchymal stromal cells

CD362, also called syndecan-2 and fibroglycan, is one of the major heparan sulfate proteoglycan-containing cell surface proteins [75]. CD362 is expressed in mesenchymal cells, including the mesenchymal cells layer surrounding the axial blood vessels in zebrafish and in cells [76] of mesenchymal origin in the kidney, lung, stomach, cartilage and bone in the mouse [77]. CD362 has been shown to play a role in cell adhesion, cell migration, cell signaling [78], and angiogenesis inhibition [79]. Syndecan-1 is thought to play an important role in myocardial infarct healing, cardiac fibrosis [80] and systolic HF [81], while syndecan-4 has been shown to regulate cardiac fibrosis and decelerate cardiac hypertrophy in HF [82]. Both syndecan-4 and syndecan-1 are up-regulated in diabetic rats with diastolic cardiac dysfunction [83]. Until now, the role of CD362 in cardiovascular diseases, especially cardiomyopathy and HF, is not yet clear.

The current criteria of the European Union focusing on MSC sterility and toxicology for defining an MSC-based Advanced Therapy Medicinal Products are limited. Meanwhile, both the European Union and the British Standard Institute highlight the BM-plating method of purifying MSCs as inadequate for defining or purifying MSC for clinical use, since only 1:100,000 BM-derived MNCs plated are MSCs. CD362 has been chosen as a maker for selecting MSCs from the mixture of BM cells by Orbsen Therapeutics Ltd (Galway, Ireland), making it possible to collect a clearly defined population of MSCs from human BM. An anti-CD362 antibody is used to select MSCs from BM at a higher MSC/MNC purity ratio of 1:13, a ratio obtained with a mixture of other antibodies. Based on the superior selecting ability of MSCs with a clearly defined population, the “Repair of Diabetic Damage by Stromal Cell Administration” (REDDSTAR) Consortium of the European Commission 7th Framework aimed to evaluate the efficacy of CD362^{+}, versus CD362^{-} and unselected BM-MSCs in alleviating diabetic cardiomyopathy, diabetic nephropathy, diabetic neuropathy, diabetic retinopathy and wound ulceration.

2. RATIONALE

Although optimal traditional treatment of type 1 DM can effectively achieve a near normal glycemic level and delay pathological progression of disease, it is still unlikely to avoid diabetes-related end-organ damage and complications such as diabetic cardiomyopathy. Given these limitations, it remains an ongoing task to identify the ideal method of treating these diabetic complications. Considering the cardiac regenerative, cardiac remodeling, and anti-inflammatory effects of MSCs on the one hand, and the necessity to evaluate the potential of $CD362^{+}$ selected MSCs on the other hand, the project of my thesis aimed to investigate the potential impact of $CD362^{+}$ versus $CD362^{-}$ and wild type BM-MSCs on diabetic cardiomyopathy in an STZ-induced type 1 DM mouse model.

3. MATERIALS AND METHODS

3.1 Materials and equipment

3.1.1 Materials

Table 4. Consumption materials

Article	Description	Company
96-well Multiply®-PCR plate		Sarstedt, Nürnbrecht, Germany
Cell Strainer	70 µm	BD Biosciences, New Jersey, USA
Coverslips	21 x 26 mm	R. Langenbrinck, Emmendingen, Germany
Cryotubes	1.5 ml	Carl Roth, Karlsruhe, Germany
Falcon tubes	15 ml, 50 ml	Corning, New York , USA
Folded filter	MN615 1/4·¢240 mm	Macherey-Nagel, Düren, Germany
Gloves		Sempercare, Northamptoshire, Germany
Masks		Charite, Berlin, Germany
MicroAmp®Optial 384-well plate	Reaction plate with Barcode	Thermo Fisher Scientific, Waltham, Massachusetts, USA
Microtome blades	A35 type	Feather, Köln, Germany
PCR-tubes	0.2 ml, conical lid	Biozym, Hess. Oldendorf, Germany
Pipette tips	10 µl, 100 µl, 1000 µl	Biozym, Hess. Oldendorf, Germany
Pipettes		Corning, New York , USA
Plastic cannulas	18G und 20G	B.Braun, Melsungen, Germany
Plunger	2.5 ml syringe	TERUMO, Tokyo, Japan
Reaction Tubes	Safe-Lock or RNAse free	Sarstedt, Nürnbrecht, Germany
Scalpels		Feather, Köln, Germany
Slides	Super Frost Plus	R.Langenbrinck, Emmendingen, Germany

3.1.2 Equipment

Table 5. Laboratory equipment

Equipment	Description/Type	Company
Conductance catheter	1.2 French	Scisense Inc., Ontario, Canada
Cryostat		Microm, Minutes nestota, USA
Homogenizer	Pellet Pestle Motor	Sigma, Taufkirchen, Germany
Horizontal shaker	SM-25	Edmund Bühler, Tübingen, Germany
Ice maker	AF-10	Scotsman, Vernon Hills, USA
Incubator	Function Line	Heraeus, Osterode, Germany
Microscope	DM2000 LED	Leica, Bensheim, Germany
MACSQuant Tyto		Miltenyi Biotec, Bergisch Gladbach, Germany
pH meter	Knick Digital 646	Beyer, Düsseldorf, Germany
Pipettes		Eppendorf, Wesseling-Berzdorf, Germany
P-V Amplifier System	MPVS 300/400	Millar Instruments, Houston, USA
Spectrophotometer	NanoDrop	Thermo Scientific PEQLAB, Erlangen, Germany
Photometer	SPECTRA max 340PC384	Molecular Devices, Biberach an der Riß, Germany
Tabletop centrifuge	Centrifuge 5415 C	Eppendorf, Wesseling-Berzdorf, Germany
Thermocycler	Mastercycler gradient	Eppendorf, Wesseling-Berzdorf, Germany
Thermomixer	Comfort	Eppendorf, Wesseling-Berzdorf, Germany
Ventilator	Minutes i-Vent	Harvard Apparatus, Massachusetts,USA
Vortexer	VF2	IKA-Labortechnik, Staufen, Germany

3.1.3 Buffer and reagent

Table 6. Buffer reagent and kits

Article	Company
1% ß-mercaptoethanol	Sigma-Aldrich Chemie GmbH, Taufkirchen, Germany
3-aminutes o-9-ethylcarbazole (AEC)	Sigma-Aldrich Chemie GmbH, Taufkirchen, Germany
Acetic acid	VWR International GmbH, Darmstadt, Germany

Acetone	VWR International GmbH, Darmstadt, Germany
Avidin-Biotin-Blocking(ABC)-Kit	Vector Labs, Burlingame, USA
Bovine serum albuminutes (BSA)	Carl Roth, Karlsruhe, Germany
Calcium chloride	VWR International GmbH, Darmstadt, Germany
Dianova (secondary antibody)	Dianova, Hamburg, Germany
Di-Sodium hydrogen phosphate dihydrate	VWR International GmbH, Darmstadt, Germany
Distilled water	Alleman Pharma GmbH, Rimbach, Germany
DNAse I	Qiagen, Hilden; Germany
EDTA	VWR International GmbH, Darmstadt, Germany
EnVision K4003	Dako, Hamburg, Germany
Ethanol	Sigma-Aldrich Chemie GmbH, Taufkirchen, Germany
Fetal Bovine Serum (FBS)	Biochrom, Berlin, Germany
Fixation/Permeabilization kit	BD Biosciences, New Jersey, USA
Formalin	Sigma-Aldrich Chemie GmbH, Taufkirchen, Germany
GLYCO-Tek Affinity Column Kit	Helena Laboratories, Texas, USA
Hemalum	VWR International GmbH, Darmstadt, Germany
High Capacity cDNA Reverse Transcription Kit	Applied Biosystems, Darmstadt, Germany
Hydrogen peroxide solution	Sigma-Aldrich Chemie GmbH, Taufkirchen, Germany
Isopropanol	Sigma-Aldrich Chemie GmbH, Taufkirchen, Germany
Kaiser's glycerol gelatin	Carl Roth, Karlsruhe, Germany
Magnesium chloride	VWR International GmbH, Darmstadt, Germany
N, N-dimethylformamide	Carl Roth, Karlsruhe, Germany
Optical 96-well Reaction Plate	Applied Biosystems, Darmstadt, Germany
Optical Adhesive film	Applied Biosystems, Darmstadt, Germany
Potassium chloride	VWR International GmbH, Darmstadt, Germany
Potassium dihydrogen phosphate	VWR International GmbH, Darmstadt, Germany
RNase-free water	Thermo Fisher Scientific, Waltham, Massachusetts, USA
RNeasy Minutes i Kit	Qiagen, Hilden; Germany
Sodium acetate	VWR International GmbH, Darmstadt, Germany

Sodium chloride	VWR International GmbH, Darmstadt, Germany
Sodium hydrogen phosphate	VWR International GmbH, Darmstadt, Germany
TaqMan®Gene Expression Master Mix (2×)	Thermo Fisher Scientific, Waltham, Massachusetts, USA
Tissue Tek	Sakura, Zoeterwoude, Netherlands
Tris-Base	Sigma-Aldrich Chemie GmbH, Taufkirchen, Germany
Tris-HCl	VWR International GmbH, Darmstadt, Germany
TRIzol Reagent	Thermo Fisher Scientific, Waltham, Massachusetts, USA
Universal PCR Master Mix	Applied Biosystems, Darmstadt, Germany

3.1.4 Primers

Table 7. Primers for Real-time polymerase chain reaction

Murine primers	Ordering number	Company, ID
α-SMA	Mm00725412_s1	Applied Biosystems, Darmstadt, Germany
Col1a1	Mm01302043_g1	Applied Biosystems, Darmstadt, Germany
Col3a1	Mm00802331_m1	Applied Biosystems, Darmstadt, Germany
IL-10	Mm00439616_m1	Applied Biosystems, Darmstadt, Germany
IL-1ß	Mm00434228_m1	Applied Biosystems, Darmstadt, Germany
L32	RT-SN2X-03	Applied Biosystems, Darmstadt, Germany
S100A8	Mm00496696_g1	Applied Biosystems, Darmstadt, Germany
S100A9	Mm00656925_m1	Applied Biosystems, Darmstadt, Germany
TGF-ß	Mm00441724_m1	Applied Biosystems, Darmstadt, Germany
TNF-α	Mm00443258_m1	Applied Biosystems, Darmstadt, Germany

3.1.5 Antibodies

Table 8. Antibodies used for the immunohistochemistry

Antibody	Company
Anti-α-SMA	Abcam, Cambridge, UK
Anti-CD4	BD Bioscience, Heidelberg, Germany

Anti-CD68	Abcam, Cambridge, Germany
Anti-CD8a	BioLegend, Koblenz, Germany
Anti-Collagen I	Merck Millipore, Darmstadt, Germany
Anti-Collagen III	Merck Millipore, Darmstadt, Germany

Table 9. Antibodies for flow cytometry

Antigen	Antibody	Company	Cat.Nr.
Annexin V	Anti-Annexin V-V450	BD Bioscience	560506
CD4	Anti-CD4 FITC	Miltenyi Biotec	130-094-164
CD8	Anti-CD8a VioBlue	Miltenyi Biotec	130-102-431
CD25	Anti-CD25 PE	Miltenyi Biotec	130-094-164
CD68	Anti-CD68 VioBlue	Miltenyi Biotec	130-102-448
FoxP3	Anti-APC	Miltenyi Biotec	130-094-164
TGF-α	Anti-TGF-α APC	BioLegend	506306
TGF-β	Anti-TGF-β APC	BioLegend	141406

3.1.6 Software

Table 10. Software

Software	Company
FlowJo 8.7. software	Tree Star, Ashland, OR, USA
GraphPad Prism 7.0	GraphPad Software, Inc., La Jolla, USA
Zotero	Zotero is a production of the Center for History and New Media at George Mason
Leica Application Suite version 4.4.0	Leica, wetzlar,Germany

3.2 Methods

3.2.1 Study design

In this experiment, 8 weeks old male C57BL6/J mice provided by Charles River (Sulzfeld, Germany) were used. Mice were randomly divided into the following groups: control (n=9), STZ (n=10), STZ WT (n=11), STZ $CD362^-$ (n=9), and STZ $CD362^+$ (n=11). After acclimatization, mice received either STZ (SIGMA-Aldrich, Munich Germany) or PBS (control animals) via intraperitoneal (i.p.) injection for five consecutive days. Four weeks post STZ, MSCs or PBS were applied via intravenous (i.v.) tail vein injection. Four weeks after MSCs or PBS application, all surviving mice were sacrificed after hemodynamic measurements. Next, blood was collected and organs were isolated.

In this experiment, blood glucose (BG) was measured weekly after 4 hour's fasting. Isolated organs, such as, heart and spleen were frozen in liquid nitrogen. All investigations were performed in accordance with the European legislation of the Care and Use of Laboratory Animals and were approved by the local authority (LaGeSo, Berlin, Germany; Registration code: G0254/13).

3.2.2 Streptozotocin-induced diabetes model establishment

3.2.2.1 Mouse strains and animal care

In this experiment, C57BL/6J mice were housed in the Forschungseinrichtung für Experimentelle Medizin (FEM; Berlin) of Charité-Universitätsklinikum Berlin with a 12-hour light/dark cycle at 19-21℃, 50-70% humidity and free access to food and water.

3.2.2.2 Streptozotocin preparation

STZ is a hydrophilic compound soluble in water, alcohol and ketone and stable at an acidic pH of 4.5. Therefore, 0.1 M citrate buffer (pH 4.5) was used to prepare a stable STZ solution. STZ in this experiment was provided by SIGMA-Aldrich CHEMIE GmbH, Steinheim, Germany.

3.2.2.3 Streptozotocin injection

After 4 hours of fasting, mice in STZ groups were i.p. injected with STZ solution at a dose of 50 mg/kg for five consecutive days (five days ahead of week 1). Control mice were injected with an equivalent volume of PBS instead.

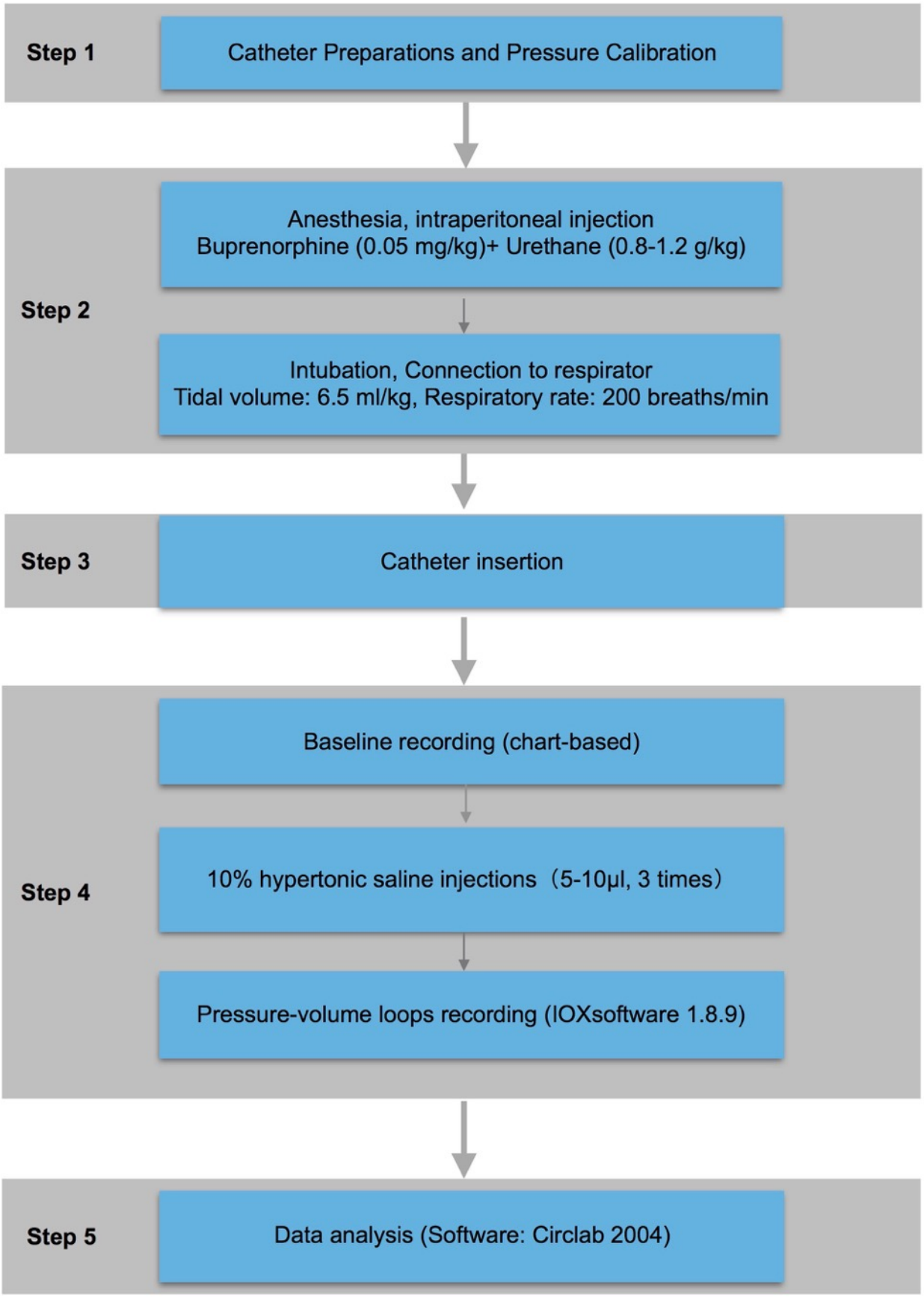

Figure 3. Main steps of hemodynamic measurement

3.2.2.4 Blood glucose monitoring and HbA1c measurement

After the initial STZ solution injections, BG levels were monitored weekly using the Accu-Chek Aviva® (Roche Diabetes Care Deutschland GmbH, Mannheim, Germany). Mice with hyperglycemia (fasting BG level ≥ 250 mg/mL) were defined as diabetic and used for the following experiments [84, 85]. Glycated hemoglobin fraction (HbA1c) was defined as the proportion of glycated hemoglobin in non-glycated hemoglobin, which was measured on the 9th week in all groups by the Helena GLYCO-Tek kit (Helena Laboratories, Texas, USA).

3.2.3 Bone marrow-derived mesenchymal stromal cell intervention

In this experiment, wild type (WT), $CD362^-$, and $CD362^+$ BM-MSCs from the same donor were provided by Orbsen Therapeutics Ltd. Four weeks after STZ application, WT, $CD362^-$, and $CD362^+$ MSCs at passage 4 with a concentration of $1x10^6$ / mouse in 200 µl PBS were i.v. injected in mice in STZ WT, STZ $CD362^-$, and STZ $CD362^+$ groups, respectively. Mice in the control and STZ groups were injected with an equivalent volume of PBS instead.

3.2.4 Catheter−based hemodynamic measurements

3.2.4.1 Measurement Procedure

Four weeks after MSCs or PBS application, all mice received a pressure-volume conductance catheter measurement under general anesthesia through apical stab according to Pacher *et al.* [86]. The main procedure steps are shown in **Figure 3**. A combination of buprenorphine and urethane was used for anesthesia by i.p. injection at a dose of 0.05mg/kg and 0.8-1.2g/kg, respectively. Anesthesia depth was checked by pain stimulus. For intubation, a 22G cannula was used, which was connected to the ventilator (Min-Vent, Harvard Apparatus, Massachusetts, USA).

The pressure-volume (PV) data of the LV were recorded in real time with conductance catheter (**Figure 4**), by which it is possible to determine both volume-dependent and -independent parameters that describe the heart function [86]. In the procedure, a 1.2 French catheter (Scisense Inc., Ontario, Canada) was placed into LV, which was connected to a pressure-volume-amplifier system (MPVS 300/400, Millar Instruments, Houston, USA). Data were collected using the software program "IOX", 1.8.9 (EMKA Technologies, Falls Church, USA) and then analyzed using the program "Circlab

2004" (Paul Steendijk, GTX Medical Software, Belgium). According to the flow chart, baseline PV loops were recorded, followed by volume calibration with hypertonic saline (10%) injection [87]. All data were acquired without ventilation for 5 seconds to avoid lung motion artifacts. The mean value of three continuous measurements of hemodynamic parameters was used in final statistical analysis. Common hemodynamic parameters assessed in PV measurement are listed in **Table 11.**

Table 11. Hemodynamic parameters

Parameter	Definition
dP/dt_{max} (mmHg/s)	The maximal rate of rise of LV pressure
dP/dt_{min} (mmHg/s)	The maximal rate of decrease of LV pressure
EF (%)	Ejection fraction, the fraction of blood volume pumped out of the LV in each cardiac cycle
LVESV (µl)	The volume of the LV at the end of systole
LVEDV (µl)	The volume of the LV at the end of diastole
LVESP (mmHg)	The pressure in the LV at the end of systole
LVEDP (mmHg)	The pressure in the LV at the end of diastole
SV (µl)	Stroke volume, the blood volume pumped from the LV into the aorta with each beat

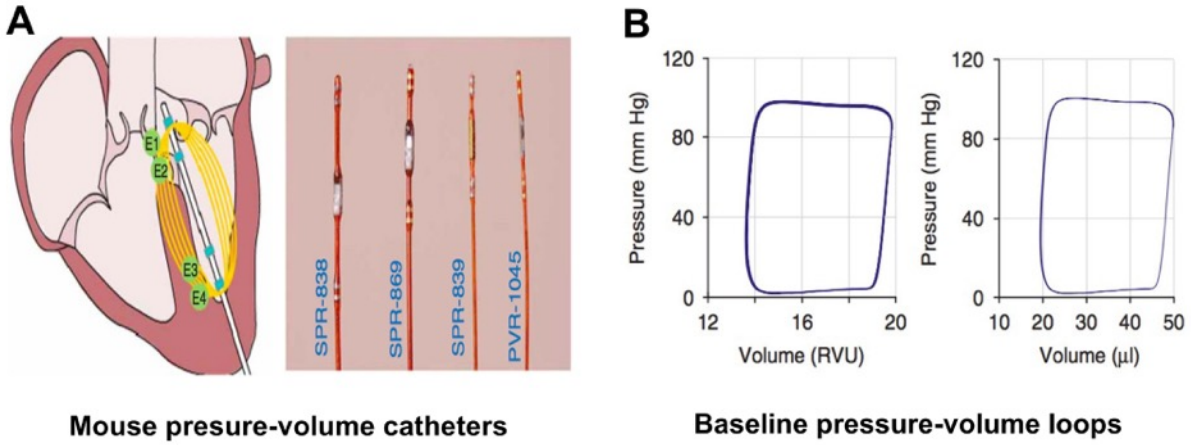

Figure 4. Mouse pressure-volume catheters (A) and representative examples of mouse baseline pressure-volume loops (B) [86]**.**

3.2.4.2 Tissue collection

After the hemodynamic measurement, mice were sacrificed and hearts and spleens were harvested for molecular and histological analyses. All tissue was immediately frozen in liquid nitrogen. Serum samples were kept frozen at -80°C.

3.2.5 Immunohistochemical analysis

Immunohistochemical analysis [88] was carried out on 5-µm-thick cryosections using antibodies listed in **Table 12**. Analysis of stained sections was made in a blinded fashion by digital image analysis on a Leica DM2000 LED microscope (Leica Microsystems, Wetzlar, Germany) at a 100x magnification.

Table 12. Antibodies used in the Immunohistochemical analysis

Primary Ab	Species	Dilution	Second Ab	Species	Dilution	Method
α-SMA	Rabbit	1:200	EnVision	Anti-Rabbit	—	EnVision
$CD4^+$	Rat	1:50	Dianova	Anti-Rat	1:250	ABC
$CD68^+$	Rabbit	1:150	EnVision	Anti-Rabbit	—	EnVision
$CD8a^+$	Rat	1:50	Dianova	Anti-Rat	1:250	ABC
Collagen I	Rabbit	1:500	EnVision	Anti-Rabbit	—	EnVision
Collagen III	Rabbit	1:200	EnVision	Anti-Rabbit	—	EnVision

3.2.5.1 Cryosections

All tissue specimens were stored at -80 °C. Before cutting, tissues were directly aligned on the stamp of the cryostat and embedded with Tissue-Tek optimum cutting temperature compound (Sakura, Zoeterwoude, The NetherLands). The frozen sections were cut on a cryostat (Microm, Minnesota, USA), and the average thickness was 5 µm. The sections were mounted on adhesive slides, dried at room temperature (RT) and subsequently stored at -20 °C.

3.2.5.2 Immunohistochemical staining

Based on antigen-antibody reactions, immunohistochemical stainings aims to detect histological antigens on sections. The antigen-specific antibody is bound to a secondary

antibody with a coupled enzyme. Further, the distribution and localization of biomarkers or differentially expressed proteins in different parts of tissue is subsequently visualized by an appropriate substrate. In this study, the Avidin-biotin complex (ABC) staining and the EnVision staining methods were used.

3.2.5.2.1 Avidin-biotin complex staining

The ABC staining is termed an immunoperoxidase method, which is based on the binding of an antibody to a suitable target antigen. The extraordinary affinity of avidin for biotin allows specific binding between biotin-containing molecules in the complex mixture and avidin. This combination of biochemistry has a stable, almost irreversible character. In this study, it was used to determine the cardiac infiltration of inflammatory cells such as $CD4^+$, $CD8a^+$ and $CD68^+$.

3.2.5.2.2 EnVision staining

EnVision staining is a two-step staining in which the application of the primary antibody is followed by a polymeric conjugate consisting of a large number of secondary antibodies (goat anti-mouse or goat anti-rabbit) bound directly to a dextran backbone containing horseradish peroxidase. One such conjugate contains up to 100 horseradish peroxidase molecules and up to 15 antibodies. Therefore, it is suitable for a variety of antibodies. EnVision has the advantage of eliminating endogenous biotin-induced nonspecific staining, with fewer steps than ABC staining. In this study, it was used to demonstrate the expression of collagen I and III, and alpha-SMA in cardiac tissue.

3.2.5.3 Digital image analysis

All tissue sections were analyzed with the color-coded digital image analysis technique through light microscopy (Leica DM2000 LED). Twenty view fields from each specimen were evaluated in a 100x magnification and digitized by a video camera. With this evaluation method, the selected fields in light microscope can be independently and accurately evaluated. The digital image processing was performed with the digital software (Leica Application Suite version 4.4.0) for which a self-programmed macro, one for areal and one for cell calculation has been developed. All microscopic images obtained for detecting the stained antigens were measured with a 100-fold microscope magnification. Quantification of collagen I, collagen III and α-SMA was expressed as

area fraction (AF) in %. The infiltration of immune cells ($CD4^+$, $CD8a^+$, $CD68^+$) was expressed in the form of positive cells/mm^2.

3.2.6 Gene expression analysis

3.2.6.1 RNA extraction

The TRIzol™ reagent (Invitrogen, Heidelberg, Germany) was used to isolate ribonucleic acid (RNA) from the LV. Frozen tissue samples in a FACS tube containing 1 ml TRIzol™ reagent were homogenized for 30 seconds, shaken for 15 seconds after adding 200 µl chloroform, and then incubated at RT for 2 minutes. Then, they were centrifuged at an accelerated speed of 10,000 rpm for 15 minutes at 4 °C and a colorless upper phase, containing the RNA, was collected. For RNA precipitation, 500µl of 100% isopropanol was added, incubated at RT for 15 minutes, and centrifuged at 10,000 rpm at 4 °C for 10 minutes. The supernatant was removed and 500 µl ethanol (70%) was added and vortexed, followed by centrifugation for 10 minutes at 4 °C and at an acceleration of 7,500 rpm. The remaining RNA pellets were dissolved in 100 µl RNase-free water and purified with the NucleoSpin® RNA mini kit (Macherey-Nagel GmbH, Düren, Germany). Samples were supplemented with 300 µl RA1 buffer and 300 µl ethanol (96%) and centrifuged at 12,000 rpm for 30 seconds followed by adding 350 µl membrane desalting buffer and a repeated centrifugation at 12,000 rpm for 1 minute. Next, 10 µl reconstituted rDNase was mixed with 90 µl reaction buffer and samples were incubated at RT for 15 minutes. Membranes were washed 3 times with 200 µl RA2, 600 µl RA3, and 250 µl RA3, respectively, and then centrifuged for 2 minutes. Finally, 50 µl RNase-free water was used to elute the RNA and centrifuged for 1 minute. The spectrophotometer (NanoDrop 1000, Thermo Scientific, Erlangen, Germany) was used to examine the concentration of RNA with absorbance at 260 nm.

3.2.6.2 Reverse Transcription

Reverse transcription from isolated RNA to complementary DNA (cDNA) was performed by the high Capacity cDNA Reverse Transcription Kit from Applied Biosystems (Darmstadt, Germany). 1 µg RNA was completed to a total volume of 11 µl RNase-free water. Random primers and template RNA were heated for 5 minutes at 70 °C in a thermocycler. Meanwhile, a master-mix was prepared by mixing the following components in one tube: 2 µl buffer + 3.2 µl RNase-free water + 1 µl reverse

transcriptase. The reaction tubes were directly put on ice and 6.2 µl of the master-mix was added. Then, the reverse transcription was performed in a thermocycler according to the following program: 10 minutes at 25 °C, 2 hours at 37 °C, followed by additionally 5 minutes at 85 °C and cool down to 4 °C. Finally, 30 µl RNase-free water was added to each sample to a final volume of 50 µl.

3.2.6.3 Real-time polymerase chain reaction

Real-time polymerase chain reaction (PCR) was performed by using a mixture of 5 µl PCR master-mix, 0.5 µl gene reporter assay, and 3.5 µl water.

The reporter assays obtained (Life Technologies GmbH, Darmstadt, Germany) included forward and reverse primers as well as the fluorescently 5' 6'FAM-labelled probe, with a 3' non-fluorescent Quencher NFQ-MGB). All primers used in this experiment are listed in Table 7. The 7900HT real-time system (Applied Biosystems, Darmstadt, Germany) was used to amplify the sample according to the following steps:

First, Prevention of carry-over contamination by addition of Uracil-DNA N-Glycosylase (UNG) for 2 minutes at 50°C. Second, denaturation and activation of the amplification-Taq DNA polymerase for a period of 10 minutes at a temperature of 95°C, and second denaturation for 15 seconds at a temperature of 95°C. Third, annealing and elongation over 1 minute at a temperature of 60°C. Depending on the target gene, second denaturation, annealing and elongation were repeated 40 or 45 times. Analysis of the collected data was performed using the SDS program 2.2.2 (Applied Biosystems, Darmstadt, Germany).

3.2.6.4 Housekeeping gene

Housekeeping genes are typically constitutive genes required to maintain essential cell functions and are expressed in all cells of the organism under normal and pathophysiological conditions [89]. In this experiment, L32 was chosen as the housekeeping gene and used for normalization of the target gene (**Figure 5**). Data were further normalized against L32, which served as an endogenous control using the 2^-ΔΔCt formula. To evaluate the n-fold change, mRNA levels in other groups were compared to the control group.

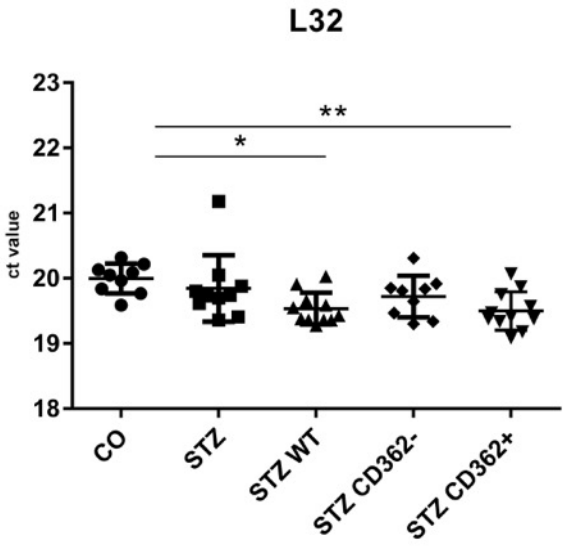

Figure 5. Housekeeping gene L32 in streptozotocin-induced diabetic mice. Bar graphs represent Ct value of L32 among CO (n=9), STZ (n=10), STZ WT (n=11), STZ $CD362^-$ (n=9) and STZ $CD362^+$ (n=11) groups. Data are expressed as mean ± SEM, P value from Kruskal-Wallis test. *p<0.05, **p<0.01. **Abbreviations:** ct= cycle threshold, STZ= streptozotocin, WT= wild type.

3.2.7 Flow cytometry analysis

3.2.7.1 Immunomodulatory effects of MSCs

Flow cytometry was used to analyze the potential immunomodulatory effects of MSCs in STZ-induced diabetic mice. Spleens from all groups in this experiment were collected and a single cell suspension was prepared. In detail, the collected spleens were positioned in a petridish containing RMPI media and mashed through a 70 µm cell strainer using the plunger of a 2.5 ml syringe. The cell strainer was then flushed with 15 ml PBS containing 1% FBS. Afterwards, the solution was centrifuged for 5 minutes at 3500 rpm and RT. The supernatant was carefully aspirated and the remaining pellet was resuspended in 6 ml ACK lysis buffer. Lysis of the erythrocytes was stopped with 40 ml RPMI after incubating for 4 minutes. Finally, the cell suspension was passed through a 40 µm cell strainer and centrifuged at RT and 3500 rpm for 5 minutes. Subsequently, the supernatant was aspirated, and the cell pellet was resuspended in FBS supplemented with 10% DMSO and stored at -80 °C for further analysis.

3.2.7.2 Splenic regulatory T cells

The mouse Tregs detection kit (Miltenyi Biotec) was used to analyze splenic regulatory T cells (Tregs) in this experiment. Furthermore, Annexin V staining was performed to analyze apoptotic Tregs. In detail, $1x10^6$ defrozen splenocytes were resuspended in 85 µl binding buffer at a dilution of 1:10. The corresponding volumes of CD4, CD25 and Annexin V V450 (BD Bioscience, Heidelberg, Germany) AB were added to the solution and incubated for 20 minutes at 4℃ in darkness. After incubation, splenocytes were washed and centrifuged (all centrifuge at 3000 rpm for 5 minutes at 4℃). After aspiration of the supernatant, cells were resuspended in 1 ml of cold freshly prepared fixation/permeabilization solution and incubated 30 minutes at 4℃ in the dark. After washing, and additional centrifugation, the cell pellet was resuspended in 80 µl of cold permeabilization buffer and then incubated for 15 minutes and then transcription factor forkhead box protein P3 (FoxP3) AB was added for further 30 minutes at 4 °C. By adding 1 ml of cold permeabilization buffer, cells were washed and then centrifuged again. The cell pellet was resuspended in a suitable volume of PBS and measured on a MACSQuant Analyzer (Miltenyi Biotec) and the FlowJo software version 8.8.6. (Tree Star Inc., USA) was used for further analysis.

3.2.7.3 Splenic cytokine production

Defrozen splenocytes were plated at a density of $1x10^6$ cells/well in 96-well U-bottom plates (n=5 wells per condition) in Iscove medium (Sigma) containing 10% FBS and 1% P/S. Cells were further stimulated with PMA/Ionomycin (BD Biosciences) at a final concentration of 50 ng/ml and 500 ng/ml in 6 ml Iscove medium. And then, 4 µl of BD GolgiStop™ (BD Biosciences) was added for every 6 ml of the stimulation media and cells were incubated overnight in the dark. The next day, cells were collected, centrifuged and washed with PBS containing 1% FBS. Afterwards, cells were incubated with 300 µl fixation/permeabilization solution (Invitrogen) for 20 minutes at 4°C. For washing the cells, 1ml BD Perm/Wash™ buffer (Invitrogen) was added and samples were centrifuged. By adding 42.5 µl BD Perm/Wash™ buffer supplemented with TGF-β AB and TNF-a AB, splenocytes were stained for 30 minutes at 4 °C in the dark. Finally after centrifugation, the cell pellet was resuspended in 200 µl PBS for flow cytometric analysis.

3.2.7.4 Splenocyte activation and proliferation

After defreezing and labeling with CFSE (CellTrace™ CFSE Cell Proliferation Kit; lifetechnologies), $1x10^6$ splenocytes were washed and centrifuged at 3000 rpm for 5 minutes. Labeled cells were plated at a density of $1x10^6$ cells/well in 96-well plates U-bottom plates (n=5 wells per condition) in Iscove medium (Sigma) containing 10% FBS and 1% P/S. Subsequently, cells were stimulated overnight with PMA/Ionomycin at a final concentration of 50 ng/ml and 500 ng/ml in 6 ml Iscove medium. One day later, CD4 and CD8 staining was performed. After additional washing and centrifugation steps, the resulting cell pellet was resuspended in 200 µl PBS for subsequent flow cytometry analysis.

3.3 Statistical analysis

Data are expressed as mean ± standard error of mean (SEM). Normality was checked by Shapiro-Wilk test. Multiple comparisons among groups were conducted by using one-way ANOVA (Bonferroni's multiple comparisons test) for normally distributed data and Kruskal-Wallis test (Dunn's multiple comparisons test) for skewed data. Analyses were performed by GraphPad Prism 7.0 (GraphPad Software, Inc., La Jolla, USA). A p value < 0.05 was considered statistically significant.

4. RESULTS

4.1 Blood glucose and HbA1c levels

BG and HbA1c levels through this experiment are listed in **Table 13**. HbA1c levels were only measured at the end of the experiment.

Table 13. Blood glucose and HbA1c levels

Parameters	Control (n=9)	STZ (n=10)	STZ WT (n=11)	STZ CD362$^-$ (n=9)	STZ CD362$^+$ (n=11)
BG (mg/dl)					
Starting	149.3 ± 5.5	151.5 ± 8.4	153.7 ± 5.4	157.0 ± 6.4	151.5 ± 6.6
Week 1	161.8 ± 10.4	187.6 ± 7.5	180.5 ± 7.6	201.9 ± 16.3	177.1 ± 7.8
Week 2	151.7 ± 6.2	350.2 ± 26.5	313.1 ± 22.7	326.4 ± 24.9	301.2 ± 19.3
Week 3	136.7 ± 6.9	411.6 ± 17.7	321.9 ± 30.7	389.7 ± 28.7	352.6 ± 18.1
Week 4	147.8 ± 8.4	447.5 ± 21.8	386.7 ± 29.0	380.8 ± 38.19	376.5 ± 30.5
Week 5	150.4 ± 5.0	451.3 ± 26.6	401.8 ± 23.8	387.7 ± 36.8	368.5 ± 24.7
Week 6	144.7 ± 7.5	395.2 ± 23.6	362.2 ± 25.2	412.0 ± 22.9	364.5 ± 25.7
Week 7	138.3 ± 3.9	437.0 ± 27.2	375.9 ± 29.6	394.3 ± 37.1	361.2 ± 27.9
Week 8	146.2 ± 7.0	409.2 ± 15.6	381.8 ± 31.7	383.6 ± 28.7	334.0 ± 21.3
Week 9	183.6 ± 8.9	467.6 ± 20.0	439.6 ± 34.0	489.4 ± 30.5	398.3 ± 33.3
HbA1c (%)	5.4 ± 0.1	10.3 ± 0.2	9.5 ± 0.3	9.2 ± 0.5	8.9 ± 0.4

Abbreviations: BG= Blood glucose, HbA1c= Hemoglobin A1c.

BG progression in mice of all experimental groups over 9 weeks from the start of the experiment followed by the STZ application and MSCs injection is shown in **Figure 6**. At the start, before the STZ injection, there was no significant difference in BG level between the control mice and the four other STZ intervention groups (all $p>0.05$). Four weeks after STZ injection, BG levels increased by 3.0-fold ($p<0.0001$), 2.7-fold ($p<0.0001$), 2.6-fold ($p<0.0001$), and 2.5-fold ($p<0.0001$) in the respective STZ, STZ WT, STZ CD362$^-$, and STZ CD362$^+$ groups, compared to control mice.

Four weeks after MSCs administration, BG levels were 2.5-fold ($p=0.0013$), 2.4-fold ($p<0.005$), 2.7-fold ($p<0.0001$), and 2.2-fold ($p<0.05$) higher in STZ, STZ WT, STZ CD362$^-$, and STZ CD362$^+$ groups compared to the control group, respectively. There

was no significant difference between STZ and the STZ-MSCs groups. Not was there a difference in BG level between the MSCs intervention groups (**Figure 7**).

Four weeks after MSCs administration, HbA1c levels were 1.9-fold ($p<0.001$), 1.8-fold ($p<0.001$), 1.7-fold ($p<0.001$), and 1.7-fold ($p<0.001$) higher in the STZ, STZ WT, STZ $CD362^-$, and STZ $CD362^+$ groups compared to the control group, respectively. There was no significant difference in HbA1c levels between STZ and the STZ-MSCs intervention groups, not between the STZ-MSCs intervention groups (**Figure 7**).

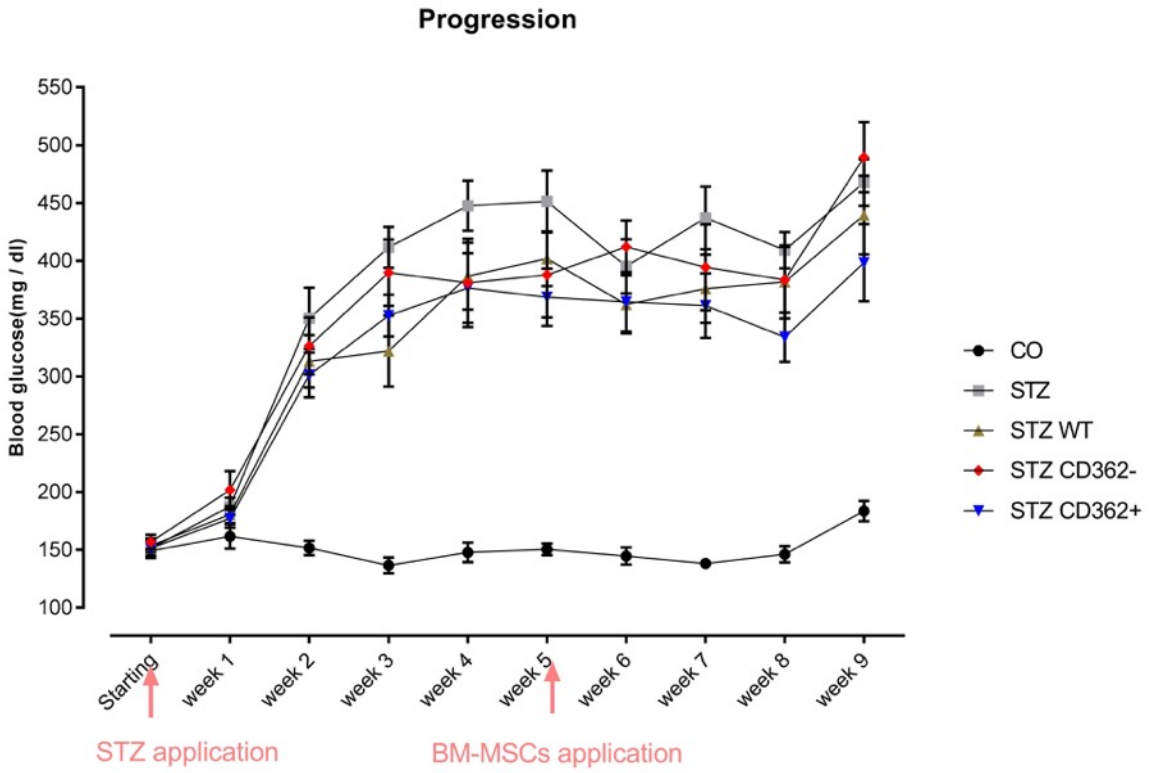

Figure 6. Blood glucose progression from baseline followed by STZ application and BM-MSCs application 4 weeks after STZ application in streptozotocin-induced diabetic mice. Abbreviations: BM= bone marrow, Co=control group, MSCs= mesenchymal stromal cells, STZ= Streptozotocin, WT= wilde type.

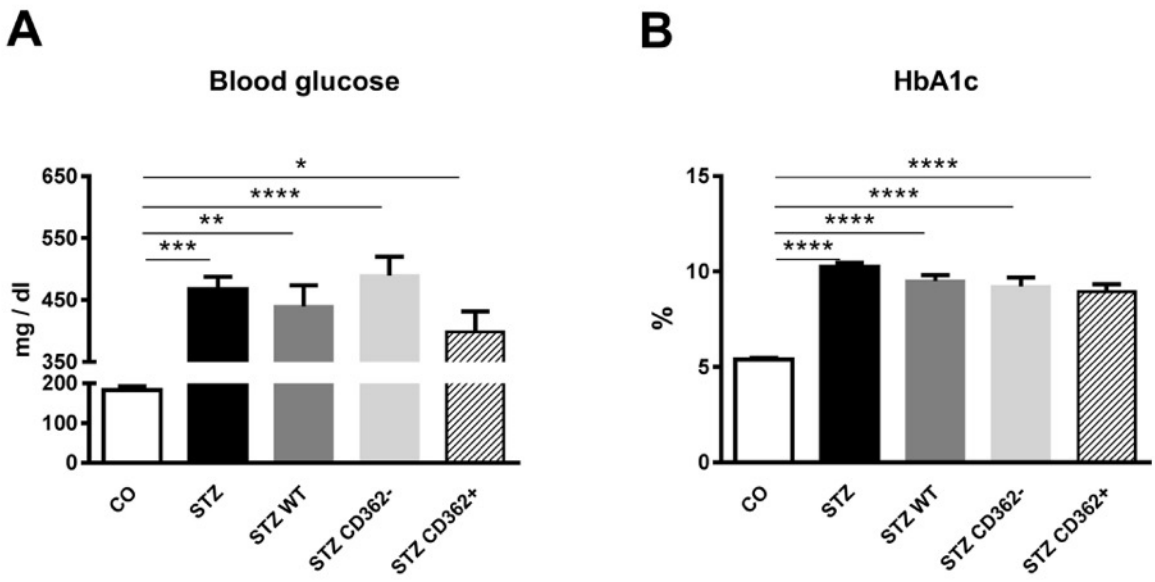

Figure 7. Blood glucose and HbA1c levels 4 weeks after stromal cell application in streptozotocin-induced diabetic mice. Bar graphs represent **A.** BG levels among CO (n=9), STZ (n=10), STZ WT (n=11), STZ CD362$^-$ (n=9) and STZ CD362$^+$ (n=11) groups. **B.** HbA1c level among groups. Data are expressed as mean ± SEM, P values are from One-way ANOVA (BG) and Kruskal-Wallis test (HbA1c). *p<0.05, **p<0.01, ***p<0.001, ****p<0.0001. **Abbreviations:** ANOVA= analysis of variance, BG= blood glucose, HbA1c= glycated hemoglobin, STZ= streptozotocin, WT= wild type.

4.2 Cardiac function parameters

The EF was 1.2-fold (p<0.05) higher in the STZ than in the control group. Four weeks after MSCs application, EF in the STZ WT, STZ CD362$^-$ and STZ CD362$^+$ groups was also not significantly different from that of the STZ group. Finally, EF was 1.2-fold (p<0.05) higher in the STZ WT than in the STZ CD362$^+$ group (**Figure 8 A**).

Furthermore, the SV was not significantly different between the STZ and the control group. Four weeks after MSCs application, SV in the STZ CD362$^+$ group was 1.3-fold (p<0.05) lower than in the STZ group. Finally, there was no difference in SV between the MSCs intervention groups (**Figure 8 E**).

The LVESV was not significantly different between the STZ and the control group. Four weeks after MSCs application, LVESV in the STZ WT, and STZ CD362$^-$ groups was also not significantly different from the STZ group. Finally, LVESV was 1.5-fold (p<0.05) higher in the STZ CD362$^+$ than in the STZ WT group (**Figure 8 B**).

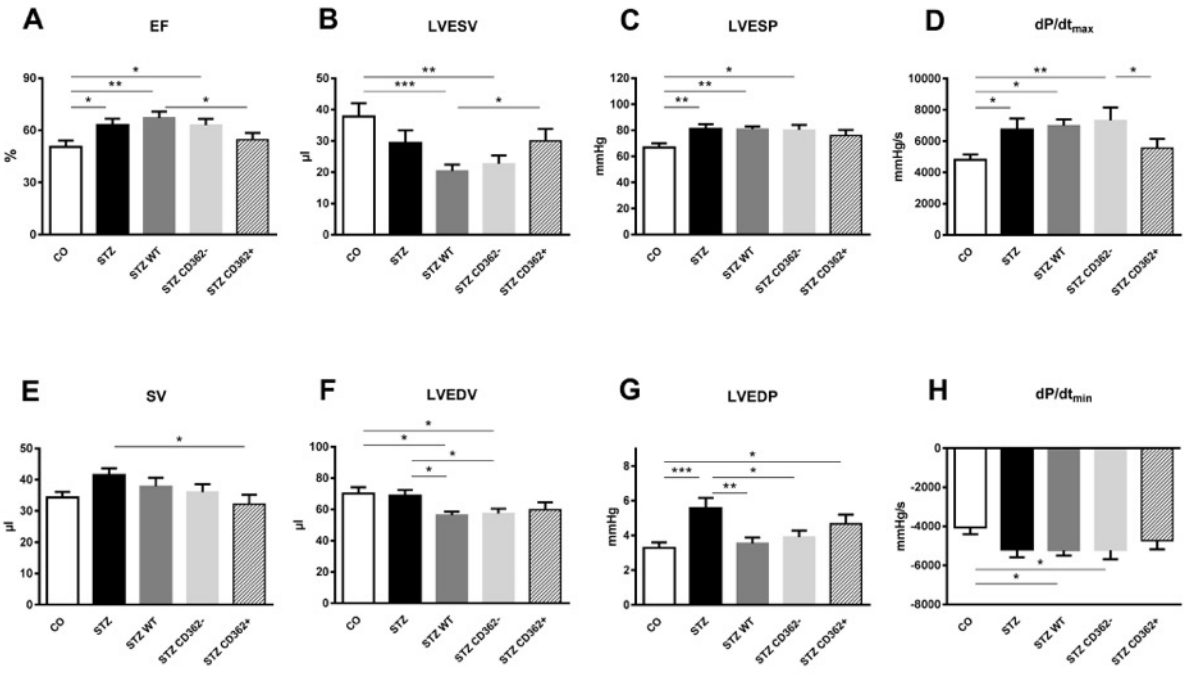

Figure 9. Cardiac function parameters 4 weeks after stromal cell application in streptozotocin-induced diabetic mice. Bar graphs represent: **A.**EF, **B.**LVESV, **C.** LVESP, **D.** dP/dt_{max} , **E.** SV, **F.** LVEDV, **G.** LVEDP, **H.** dP/dt_{min} in CO (n=9), STZ (n=10), STZ WT (n=11), STZ $CD362^-$ (n=9) and STZ $CD362^+$ (n=11) groups. Data are expressed as mean ± SEM, p values are from One-way-ANOVA, *p<0.05, **p<0.01, ***p<0.001. **Abbreviations:** ANOVA= analysis of variance, CO= control group, dP/dt_{max} = the maximum rate of the rise of LV pressure, dP/dt_{min} = the maximal rate of decrease of LV pressure, EF= ejection fraction, LVEDV= the volume of the left ventricle at the end of diastole, LVEDP= left ventricle pressure at the end of diastole, LVES = the pressure in the left ventricle at the end of systole, LVESV= the volume of the left ventricle at the end of systole, STZ= streptozotocin, SV= stroke volume, WT= wild type.

The LVEDV was not significantly different between the STZ and the control group. Four weeks after MSCs application, LVEDV in the STZ WT and STZ $CD362^-$ groups was 1.2-fold ($p<0.05$) and 1.2-fold ($p<0.05$) lower compared to the STZ group, respectively. Finally, there was no difference in LVEDV between MSCs intervention groups (**Figure 8 F**).

The LVESP was significantly 1.2-fold ($p<0.05$) higher in the STZ than in the control group. Four weeks after MSCs application, LVESP in the STZ WT, and STZ $CD362^-$ group was not significantly different from that of the STZ group. Finally, there was no difference in LVESP between the MSCs intervention groups (**Figure 8 C**).

The LVEDP was 1.7-fold ($p=0.0010$) higher in the STZ than in the control group. Four weeks after MSCs application, LVEDP was 1.6-fold ($p<0.01$) and 1.4-fold ($p<0.05$) lower in the STZ WT, and STZ $CD362^-$ groups compared to the STZ group, respectively.

Finally, there was no difference in LVEDP between MSCs intervention groups (**Figure 8 G**).

The dP/dt_{max} was 1.4-fold ($p<0.05$) higher in the STZ than in the control group. Four weeks after MSCs application, dP/dt_{max} in the STZ WT, and STZ $CD362^-$ groups was not significantly different from that of the STZ group. Finally, dP/dt_{max} was 1.3-fold ($p<0.05$) higher in the STZ $CD362^-$ than in the STZ $CD362^+$ group (**Figure 8 D**).

The dP/dt_{min} was not significantly different between the STZ and the control group. Four weeks after MSCs application, dP/dt_{min} in the STZ WT and STZ $CD362^-$ groups was not significantly different from that of the STZ group either. Finally, there was no difference in dP/dt_{min} between the MSCs intervention groups (**Figure 8 H**).

4.3 Left ventricle fibrosis

4.3.1 Gene expression

LV collagen 1a1 (col1a1) mRNA expression was not increased in STZ compared to control mice. Four weeks after MSC application, LV col1a1 mRNA expression was not different in the STZ WT, STZ $CD362^-$ and STZ $CD362^+$ groups compared to the STZ group either, nor was there a difference in col1a1 mRNA expression between the MSCs intervention groups (**Figure 9 A**). However, col1a1 mRNA expression was 1.6-fold ($p<0.01$), 1.6-fold ($p<0.01$) and 1.4-fold ($p<0.05$) increased in STZ WT, STZ $CD362^-$ and STZ $CD362^+$ mice, respectively, compared to control mice.

LV collagen 3a1 (col3a1) mRNA expression was not significantly different between the STZ and the control group. Four weeks after MSCs application, there was no difference in LV col3a1 mRNA expression in the STZ WT, STZ $CD362^-$ and STZ $CD362^+$ groups compared to the STZ group, nor was there a difference in col3a1 between the MSCs intervention groups (**Figure 9 B**).

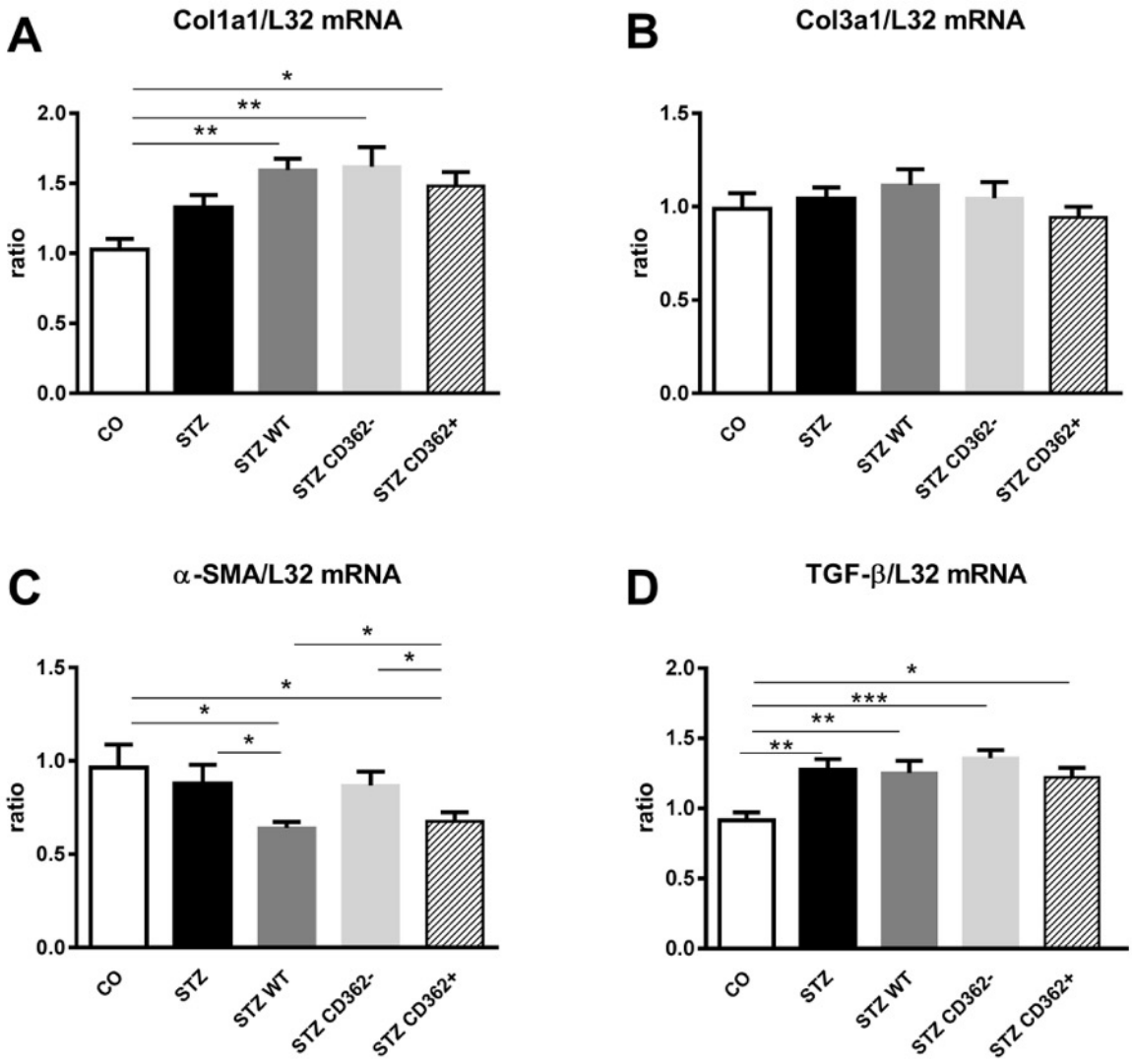

Figure 9. Collagen I, III, α-SMA and TGF-β mRNA expression in the left ventricle 4 weeks after stromal cell application in streptozotocin-induced diabetic mice. Bar graphs represent: **A.** α-1 collagen I, **B.** α-1 collagen III, **C.** α-SMA, **D.** TGF-β mRNA expression in CO (n=9), STZ (n=10), STZ WT (n=11), STZ CD362$^-$ (n=9) and STZ CD362$^+$ (n=11) groups. Data are expressed as mean ± SEM, p values are from One-way-ANOVA (collagen I and TGF-β) and from Kruskal-Wallis test. (collagen III and α-SMA) *p<0.05, **p<0.01, ***p<0.001. **Abbreviations:** ANOVA= analysis of variance, α-SMA= Alpha-smooth muscle actin, Col1a1= alpha-1 type I collagen, Col3a1= alpha-1 type 3 collagen, STZ= streptozotocin, TGF-β=transforming growth factor β, WT= wild type.

Also, LV α-SMA mRNA expression was not significantly different between STZ and control mice. Four weeks after MSC application, LV α-SMA mRNA expression was 1.4-fold ($p<0.05$) and 1.3-fold ($p=0.0587$) lower in STZ WT and STZ CD362$^+$ mice compared to STZ mice, respectively. Furthermore, LV α-SMA mRNA expression in STZ

CD362$^-$ was 1.4-fold ($p<0.05$) and 1.3-fold ($p<0.05$) higher compared to STZ WT and STZ CD362$^+$ groups, respectively (**Figure 9 C**).

LV TGF-β mRNA expression was 1.4-fold ($p<0.01$) higher in STZ than in control mice. Four weeks after MSC application, there was neither a difference in LV TGF-β mRNA expression in the STZ WT, STZ CD362$^-$ and STZ CD362$^+$ groups compared to the STZ group, nor was there a difference in TGF-β between the MSC intervention groups. However, TGF-β mRNA expression was 1.4-fold ($p<0.01$), 1.5-fold ($p<0.001$) and 1.3-fold ($p<0.05$) higher in STZ WT, STZ CD362$^-$ and STZ CD362$^+$ mice, respectively, compared to control mice (**Figure 9 D**).

4.3.2 Immunohistological evidence

4.3.2.1 Extracellular matrix protein collagen I expression

The mean AF of extracellular matrix protein collagen I expression in the control, STZ, STZ WT, STZ CD362$^-$, and STZ CD362$^+$ groups was 9.2±1.1%, 9.3±1.8%, 7.0±0.6%, 10.2±0.8% and 8.6±0.7% per mm^2 heart area, respectively.

In line with the LV col1a1 mRNA expression data, LV collagen I expression was not significantly different between the STZ and the control group. Four weeks after MSCs application, collagen I expression in the STZ WT, STZ CD362$^-$ and STZ CD362$^+$ groups was also not significantly different from the STZ group. Finally, there was no difference in collagen I protein expression between the MSCs intervention groups (**Figure 10**).

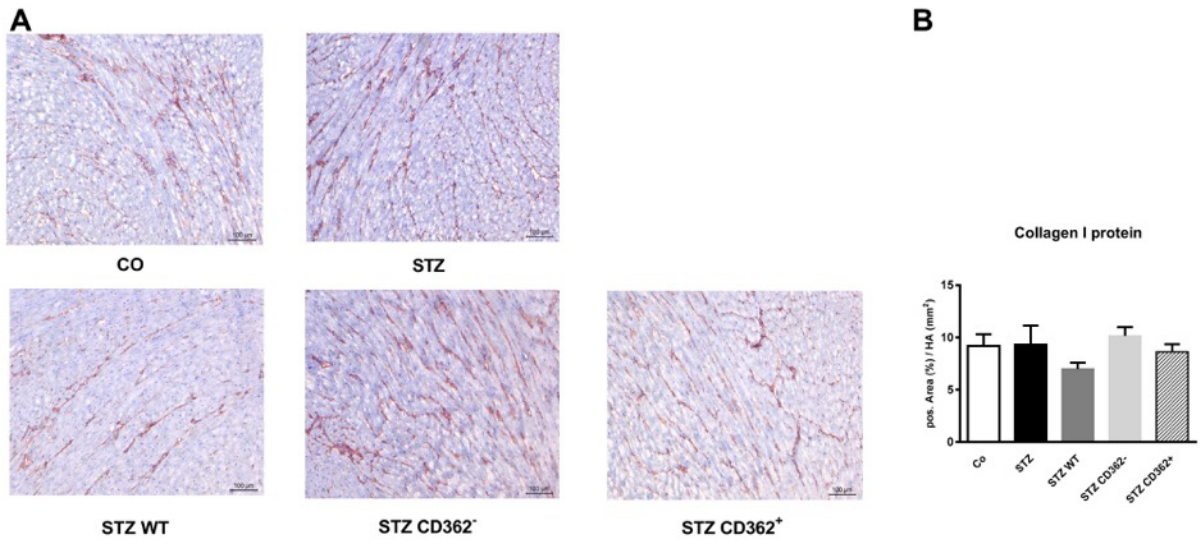

Figure 10. Collagen I expression in the left ventricle 4 weeks after stromal cell application in streptozotocin-induced diabetic mice. A. Representative collagen I expression in LV sections of CO (n=9), STZ (n=10), STZ WT (n=11), STZ CD362$^-$ (n=9) and STZ CD362$^+$ (n=11) groups, at 100x magnification. **B.** Bar graphs represent AF of LV collagen I protein expression (area / HA mm^2) among groups. Data are expressed as mean ± SEM, p values are from One-way-ANOVA. *p<0.05. **Abbreviations:** AF= area fraction, ANOVA= analysis of variance, HA= heart area, LV=left ventricle, STZ= streptozotocin, WT= wild type.

4.3.2.2 Extracellular matrix protein collagen III expression

The mean AF of extracellular matrix protein collagen III expression in the LV of control, STZ, STZ WT, STZ CD362$^-$, and STZ CD362$^+$ mice was 13.1±1.6%, 16.3±1.1%, 19.6±1.1%, 23.8±0.8% and 21.7±1.5% per mm^2 heart area, respectively.

LV collagen III expression was not significantly different between the STZ and the control group. However, LV collagen III expression was 1.5-fold (p<0.01) and 1.3-fold in (p<0.05) higher in the STZ CD362$^-$ and STZ CD362$^+$ groups versus the STZ group, respectively, There was no difference in LV collagen III protein expression between the MSCs intervention groups (**Figure 11**).

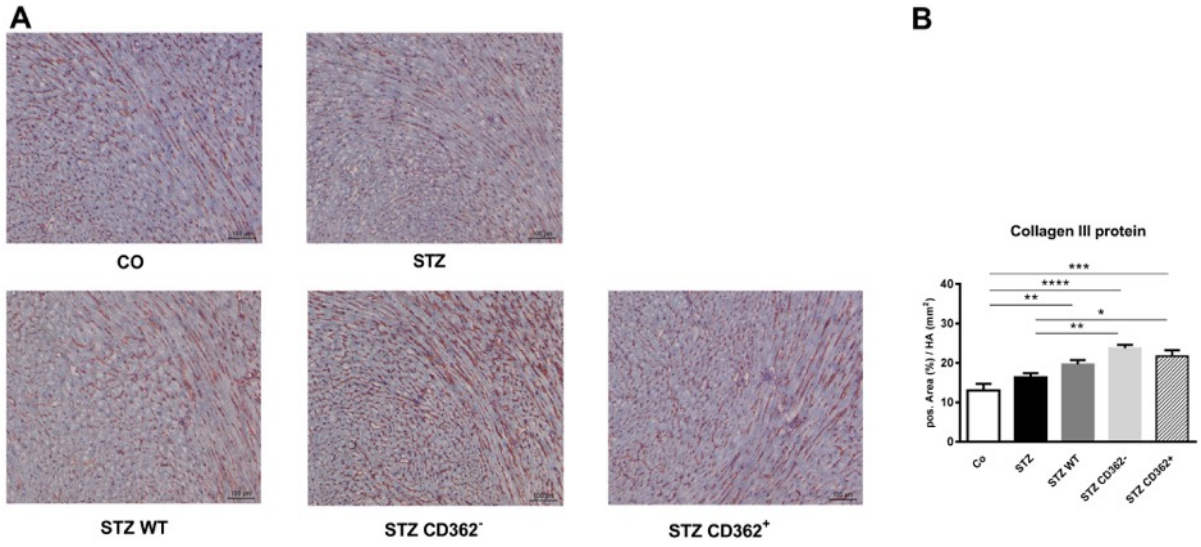

Figure 11. Collagen III expression in the left ventricle 4 weeks after stromal cell application in streptozotocin-induced diabetic mice. A. Representative collagen III expression in LV sections of CO (n=9), STZ (n=10), STZ WT (n=11), STZ CD362$^-$ (n=9) and STZ CD362$^+$ (n=11) groups, at 100x magnification. **B.** Bar graphs represent AF of LV collagen III protein expression (area / HA mm^2) among groups. Data are expressed as mean ± SEM, p values are from One-way-ANOVA. *p<0.05, **p<0.01, ***p<0.001, ****p<0.0001. **Abbreviations:** AF= area fraction, ANOVA= analysis of variance, HA= heart area, LV= left ventricular, STZ= streptozotocin, WT= wild type.

4.3.2.3 Alpha-smooth muscle actin protein expression

The mean AF of α-SMA protein expression in the LV of control, STZ, STZ WT, STZ CD362$^-$, and STZ CD362$^+$ groups was 0.36±0.03%, 0.34±0.02%, 0.41±0.04%, 0.34±0.03% and 0.37±0.03% per mm^2 heart area, respectively.

LV α-SMA expression was not significantly different between the STZ and the control group. Also, LV α-SMA expression in STZ WT, STZ CD362$^-$ and STZ CD362$^+$ mice was not significantly different from the STZ group. There was no difference in LV α-SMA protein expression between the MSCs intervention groups (**Figure 12**).

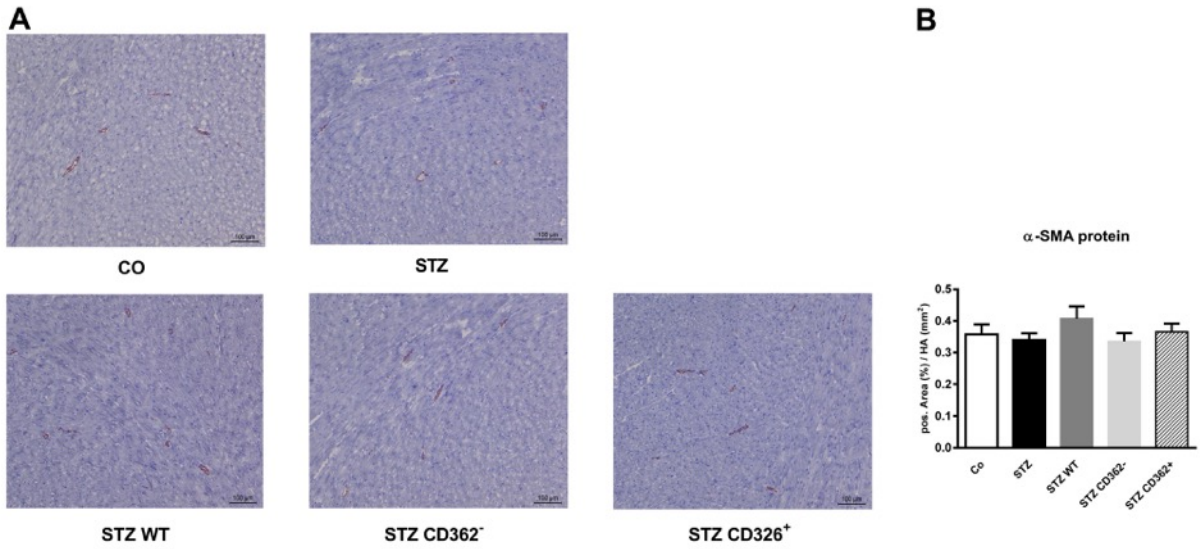

Figure 12. α-SMA expression in the left ventricle 4 weeks after stromal cell application in streptozotocin-induced diabetic mice. **A.** Representative α-SMA in LV sections of CO (n=9), STZ (n=10), STZ WT (n=11), STZ CD362$^-$ (n=9) and STZ CD362$^+$ (n=11) groups, at 100x magnification. **B.** Bar graphs represent mean AF of LV α-SMA protein expression (area / HA mm^2) among groups. Data are expressed as mean ± SEM, p value from Kruskal-Wallis test. *p<0.05. **Abbreviations:** AF= area fraction, α-SMA= alpha-smooth muscle actin, HA= heart area, LV= left ventricle, STZ= streptozotocin, WT= wild type.

4.4 Left ventricle inflammation

4.4.1 Gene expression

LV IL-1β mRNA expression was not significantly different between the STZ and the control group. Four weeks after MSCs application, LV IL-1β mRNA expression in the STZ WT, STZ CD362$^-$ and STZ CD362$^+$ groups was not significantly different from the

STZ group and there was no difference in LV IL-1β mRNA expression between the MSCs intervention groups (**Figure 13 A**).

LV TNF-α mRNA expression was not significantly different between the STZ and the control groups (p=0.0506). Four weeks after MSCs administration, LV TNF-α mRNA expression in STZ CD362^{-} mice was 1.3-fold (p=0.0551), 1.6-fold (p=0.0010), and 1.4-fold (p<0.05) higher than in STZ, STZ WT and STZ CD362^{+} mice, respectively, **(Figure 13 B).**

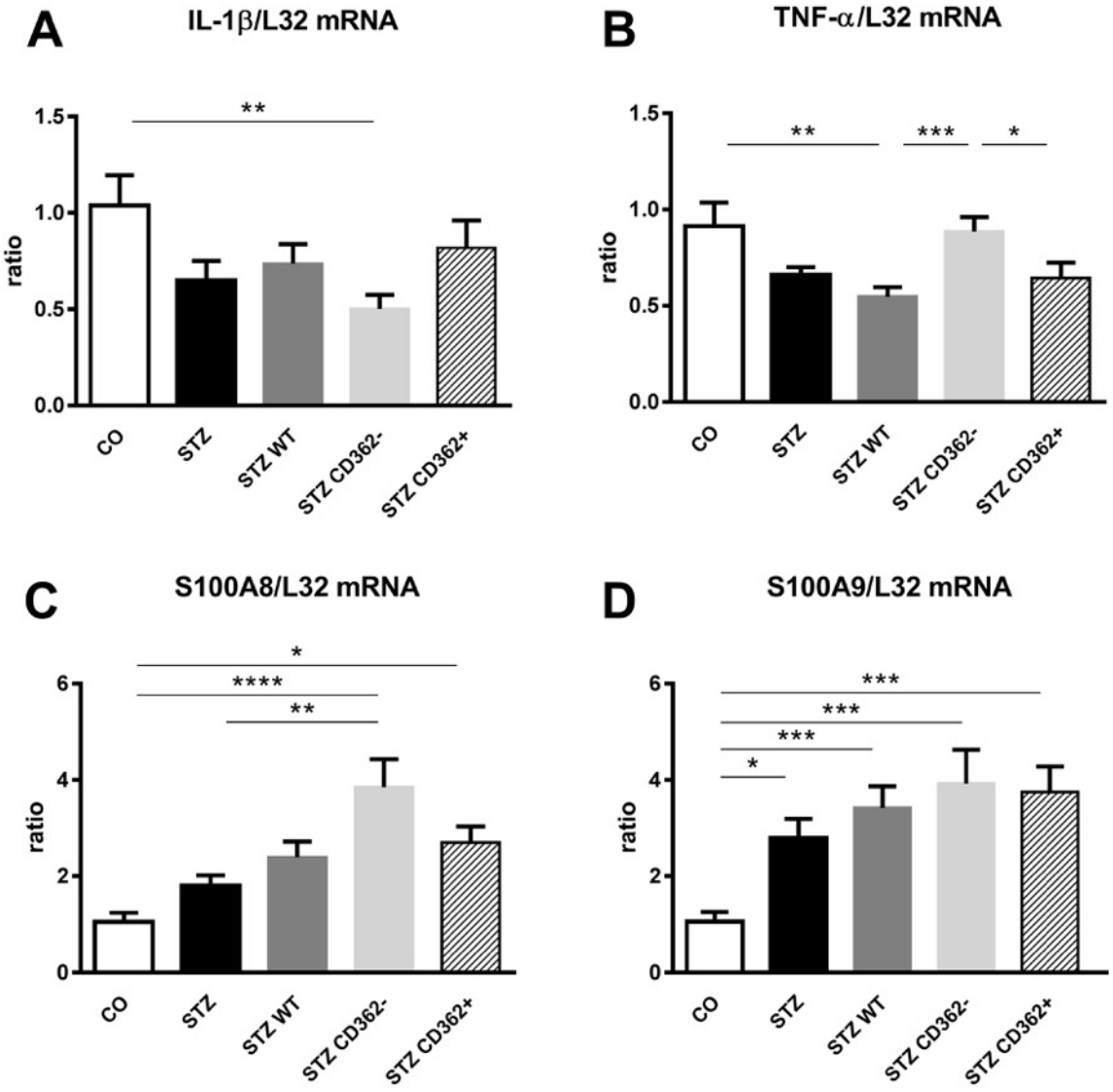

Figure 13. Cytokine and S100A8/A9 mRNA expression in the left ventricle 4 weeks after stromal cell application in streptozotocin-induced diabetic mice. Bar graphs represent: **A.** IL-1β. **B.** TNF-α. **C.** S100A8. **D.** S100A9 mRNA expression in CO (n=9), STZ (n=10), STZ WT (n=11), STZ CD362$^-$ (n=9) and STZ CD362$^+$ (n=11) groups. Data are expressed as mean ± SEM, p value from One-way-ANOVA (S100A8) Kruskal-Wallis test (IL-1β,TNF-α and S100A9). *p<0.05, **p<0.01, ***p<0.001, ****p<0.0001. **Abbreviations:** ANOVA= analysis of variance, IL-1β= Interleukin-1β, S100A8= S100 calcium-binding protein A8, S100A9= S100 calcium-binding protein A9, STZ= streptozotocin, TNF-α = Tumor necrosis factor alpha, WT= wild type.

LV S100 calcium-binding protein A8 (S100A8) mRNA expression was not significantly different between the STZ and the control group. Four weeks after MSCs administration, LV S100A8 mRNA expression in the STZ CD362$^-$ was 2.1-fold, 1.6-fold higher than the STZ (p<0.01), and the STZ WT (p=0.0699) groups (**Figure 13 C**).

S100 calcium-binding protein A9 (S100A9) mRNA expression was 2.6-fold (p<0.05) higher in the STZ than in the control group. Four weeks after MSCs injection, LV S100A9 mRNA expression was not significantly different in the STZ WT, STZ CD362$^-$ and STZ CD362$^+$ groups versus the STZ group. There was no difference in LV S100A9 mRNA expression among the MSCs intervention groups **(Figure 13 D).**

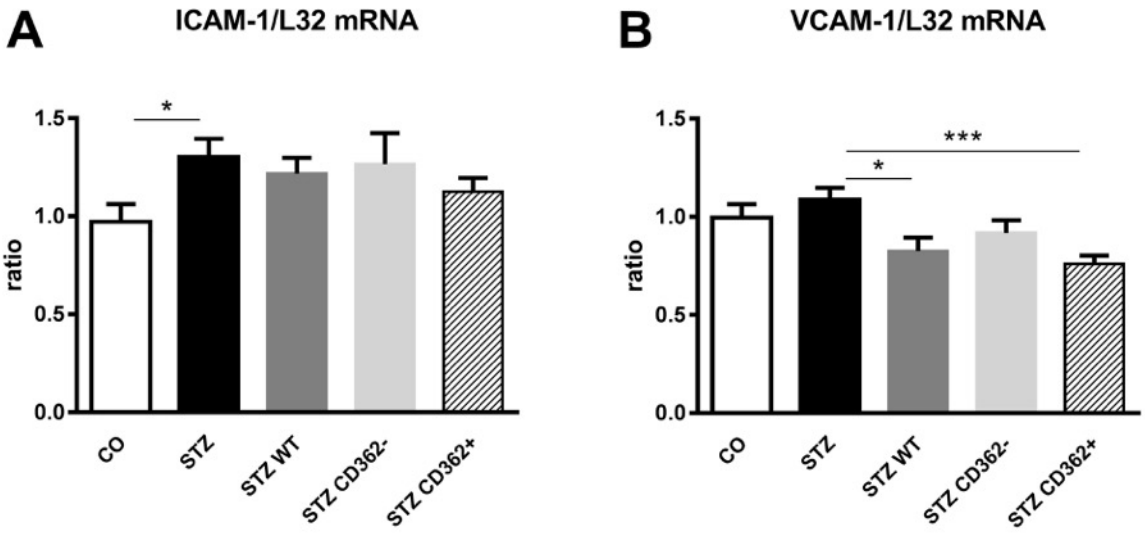

Figure 14. ICAM-1 and VCAM-1 mRNA expression in the left ventricle 4 weeks after stromal cell application in streptozotocin-induced diabetic mice. Bar graphs represent: **A.** ICAM-1. **B.** VCAM-1 mRNA expression in CO (n=9), STZ (n=10), STZ WT (n=11), STZ CD362$^-$ (n=9) and STZ CD362$^+$ (n=11) groups. Data are expressed as mean ± SEM, p value from One-way-ANOVA (VCAM-1) and Kruskal-Wallis test (ICAM-1). *p<0.05, ***p<0.001. **Abbreviations:** ANOVA= analysis of variance, ICAM-1 = intercellular adhesion molecule 1, STZ= streptozotocin, VCAM-1 = vascular cell adhesion molecule 1, WT= wild type.

Intercellular adhesion molecule 1 (ICAM-1) mRNA expression in the LV was 1.4-fold (p<0.05) higher in the STZ than the control group. Four weeks after MSCs administration, LV ICAM-1 mRNA expression was not significantly different in the STZ WT, STZ CD362$^-$ and STZ CD362$^+$ groups compared to the STZ group. Furthermore, there was no difference in LV ICAM-1 mRNA expression between the MSCs intervention groups (**Figure 14 A**).

Vascular cell adhesion molecule 1 (VCAM-1) mRNA expression in the LV was not significantly different between the STZ and the control group. Four weeks after MSCs injection, LV VCAM-1 mRNA expression was 1.3-fold (p<0.05) and 1.4-fold (p<0.001) lower in the STZ WT and STZ CD362$^+$ groups than the STZ group. There was no difference in VCAM-1 mRNA expression between the MSCs intervention groups (**Figure 14 B**).

4.4.2 Immunohistological evidence

4.4.2.1 CD4$^+$ T lymphocytes

The mean count of CD4$^+$ T lymphocytes in control, STZ, STZ WT, STZ CD362$^-$, and STZ CD362$^+$ groups was 0.9±0.2, 0.9±0.1, 1.2±0.15, 0.8±0.4 and 1.0±0.6 per mm^2 heart area, respectively.

The count of CD4$^+$ T lymphocytes was not significantly different between the STZ and the control group. Also, the count of CD4$^+$ T cells in the STZ WT, STZ CD362$^-$ and STZ CD362$^+$ groups was not significantly different from the STZ group. There was no difference in count of CD4$^+$ T lymphocytes between the MSCs intervention groups (**Figure 15**).

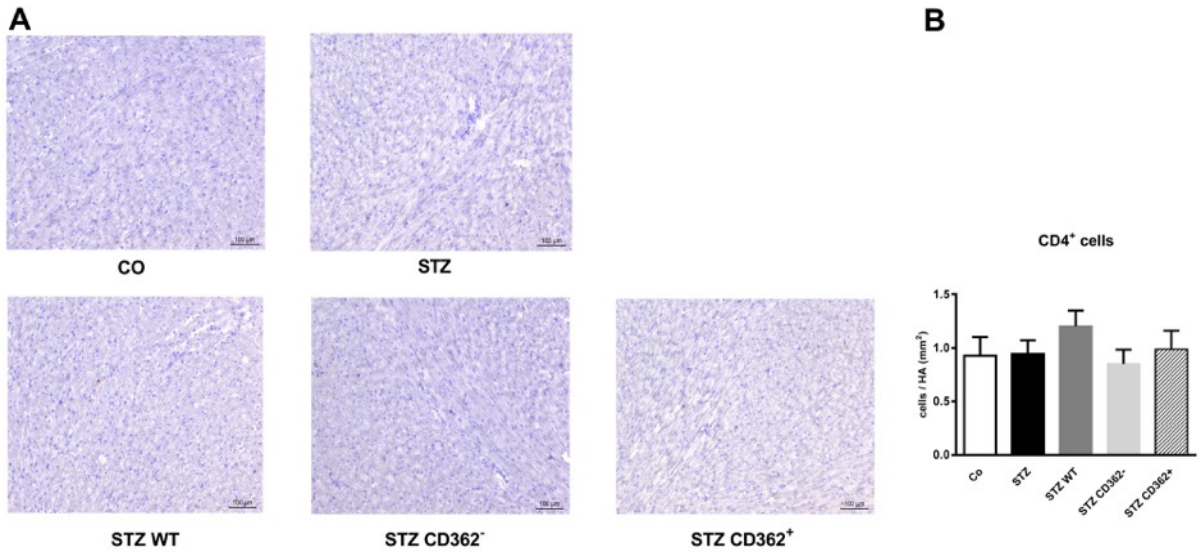

Figure 15. CD4⁺ T lymphocytes in left ventricle 4 weeks after stromal cell application in streptozotocin-induced diabetic mice. A. Representative CD4⁺ cells in LV sections of CO (n=9), STZ (n=10), STZ WT (n=11), STZ CD362⁻ (n=9) and STZ CD362⁺ (n=11) groups, at 100x magnification. **B.** Bar graphs represent the mean count of CD4⁺ cell (area / HA mm^2) of the groups. Data are expressed as mean ± SEM, p values are from One-way-ANOVA. *p<0.05. **Abbreviations:** ANOVA= analysis of variance, HA= heart area, LV=left ventricle, STZ= streptozotocin, WT= wild type.

4.4.2.2 CD8a⁺ cytotoxic T lymphocytes

The mean count of CD8a⁺ cytotoxic T lymphocytes in control, STZ, STZ WT, STZ CD362⁻, and STZ CD362⁺ groups was 0.27±0.04, 0.23±0.04, 0.41±0.06, 0.34±0.07 and 0.26±0.02 per mm^2 heart area, respectively.

The count of CD8a⁺ cells was not significantly different between the STZ and the control group, whereas the count of CD8a⁺ cells in the STZ WT group was 1.8-fold ($p<0.05$) higher than in the STZ group. The count of CD8a⁺ cells in the STZ CD362⁺ group was 1.6-fold ($p<0.05$) lower than in STZ WT group (**Figure 16**).

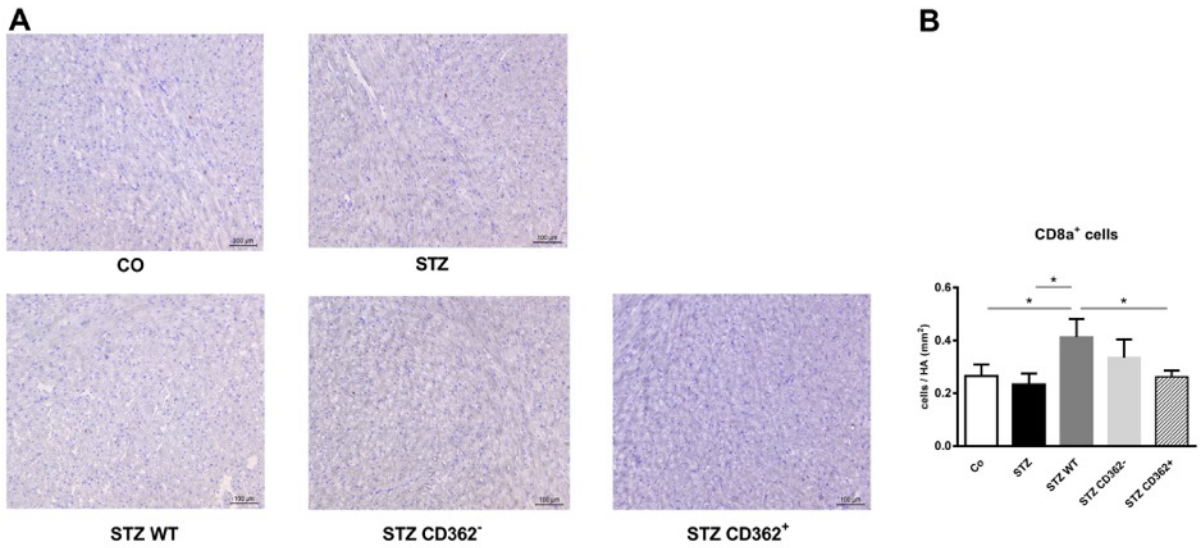

Figure 16. CD8a$^+$ cytotoxic T lymphocytes in left ventricle 4 weeks after stromal cell application in streptozotocin-induced diabetic mice. A. Representative CD8a$^+$ cells in LV sections of CO (n=9), STZ (n=10), STZ WT (n=11), STZ CD362$^-$ (n=9) and STZ CD362$^+$(n=11) groups, at 100x magnification. **B.** Bar graphs represent the mean count of CD8a$^+$ cell (area / HA mm^2) of the groups. Data are expressed as mean ± SEM, p values are from One-way-ANOVA. *p<0.05 **Abbreviations:** ANOVA= analysis of variance, HA= heart area, LV=left ventricle, STZ= streptozotocin, WT= wild type.

4.4.2.3 CD68$^+$ monocytes/macrophages

The mean account of CD68$^+$ monocytes / macrophages in the LV of control, STZ, STZ WT, STZ CD362$^-$ and STZ CD362$^+$ groups was 79.0±9.5, 74.2±10.4, 72.8±5.7, 96.9±16.3 and 125.0±14.0 per mm^2 heart area, respectively.

The count of CD68$^+$ cells was not significantly different between the STZ and the control group, whereas the amount of CD68$^+$ cells in the STZ CD362$^+$ group was 1.7-fold (p<0.01) higher than in the STZ group. The count of CD68$^+$ cells in the STZ CD362$^+$ group was 1.7-fold (p<0.05) higher than in STZ WT group (**Figure 17**).

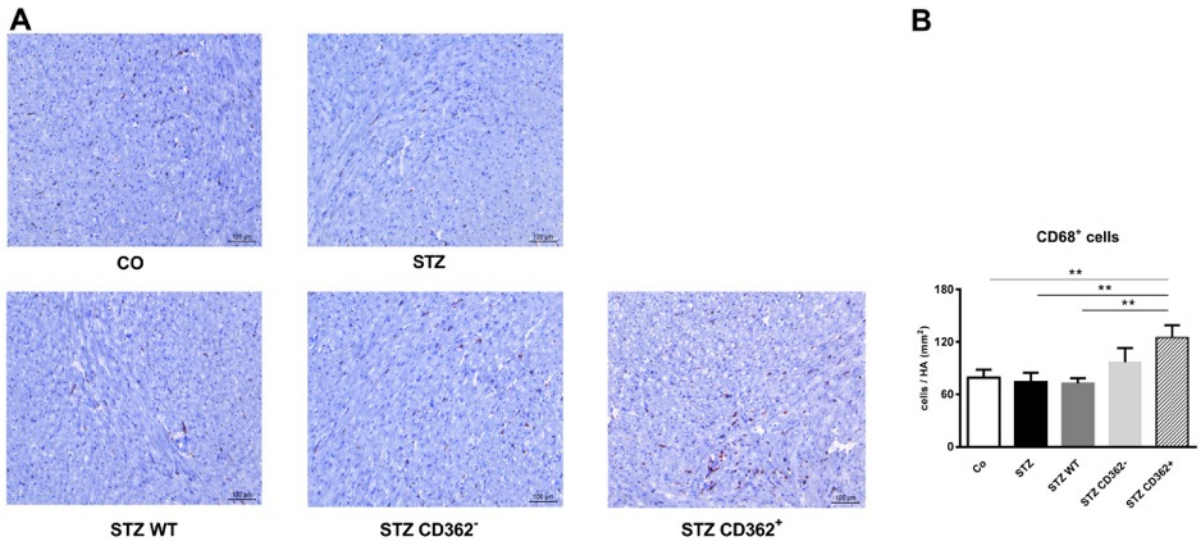

Figure 17. CD68⁺ monocytes/macrophages in left ventricle 4 weeks after stromal cell application in streptozotocin-induced diabetic mice. A. Representative CD68⁺ cells in LV sections of CO (n=9), STZ (n=10), STZ WT (n=11), STZ CD362⁻ (n=9) and STZ CD362⁺ (n=11) groups, at 100x magnification. **B.** Bar graphs represent mean the mean count of CD68⁺ cell (area / HA mm^2) of the groups. Data are expressed as mean ± SEM, p value from One-way-ANOVA. **p<0.01. **Abbreviations:** ANOVA= analysis of variance, HA= heart area, LV=left ventricle, STZ= streptozotocin, WT= wild type.

4.5 Immune regulation of splenocytes

The percentage of TNF-α-expressing CD68 cells in control, STZ, STZ WT, STZ CD362⁻ and STZ CD362⁺ groups was 1.030±0.059, 1.464±0.109, 3.324±0.268, 2.558±0.108, 2.142±0.382, respectively. The percentage of CD68⁺TNF- α⁺ cells was not significantly different between the control and STZ groups, whereas the percentage of CD68⁺TNF-α⁺ cells was 2.3-fold (p<0.0001) and 1.7-fold (p<0.05) higher in the STZ WT and STZ CD362⁻ groups compared to the STZ group, respectively. Furthermore, the percentage of CD68⁺TNF-α⁺ cells was 1.6-fold (p<0.05) higher in the STZ WT than in the STZ CD362⁺ group, respectively (**Figure 18 A**).

The percentage of TGF-ß-expressing CD68 cells in control, STZ, STZ WT, STZ CD362⁻ and STZ CD362⁺ groups was 0.192±0.073, 0.418±0.029, 0.069±0.003, 0.828±0.058, and 0.092±0.020, respectively. The percentage of TGF-ß-expressing CD68 cells was 2.2-fold (p<0.05) higher in the STZ than in the control group. Furthermore, the percentage of TGF-ß-expressing CD68 cells was 2.0-fold (p<0.0001) higher in the STZ CD362⁻ group versus the STZ group, but 6.0-fold (p=0.0001) and 4.5-fold (p=0.0003)

lower in the STZ WT and STZ CD362^{+} groups compared to the STZ group, respectively (**Figure 18 B**).

The percentage of Tregs in control, STZ, STZ WT, STZ CD362^{-} and STZ CD362^{+} groups was 0.148±0.016, 0.162±0.009, 0.156±0.009, 0.266±0.014, and 0.212±0.009, respectively. The percentage of Tregs was not significantly different between the STZ and the control group. From the different MSC STZ groups, the percentage of Tregs was significantly different only in the STZ CD362^{-} versus the STZ group. Furthermore, the percentage of Tregs was 1.7-fold ($p<0.0001$) and 1.4-fold ($p<0.05$) higher in the STZ CD362^{-} and STZ CD362^{+} mice than in the STZ WT mice, respectively, and the percentage of Tregs was 1.3-fold ($p<0.05$) higher in the STZ CD362^{-} than in the STZ CD362^{+} group (**Figure 18 C**).

The percentage of apoptotic Tregs in control, STZ, STZ WT, STZ CD362^{-} and STZ CD362^{+} groups was 37.84±3.901, 43.2±2.494, 45.08±3.166, 50.6±2.578, and 46.96±2.305, respectively. The percentage of apoptotic Tregs was not significantly different between the STZ and control groups. The percentage of apoptotic Tregs was not significantly different in the STZ WT, STZ CD362^{-} and STZ CD362^{+} groups compared to the STZ group either, not was there a difference in the percentage of apoptotic Tregs among the MSCs intervention groups **(Figure 18 D).**

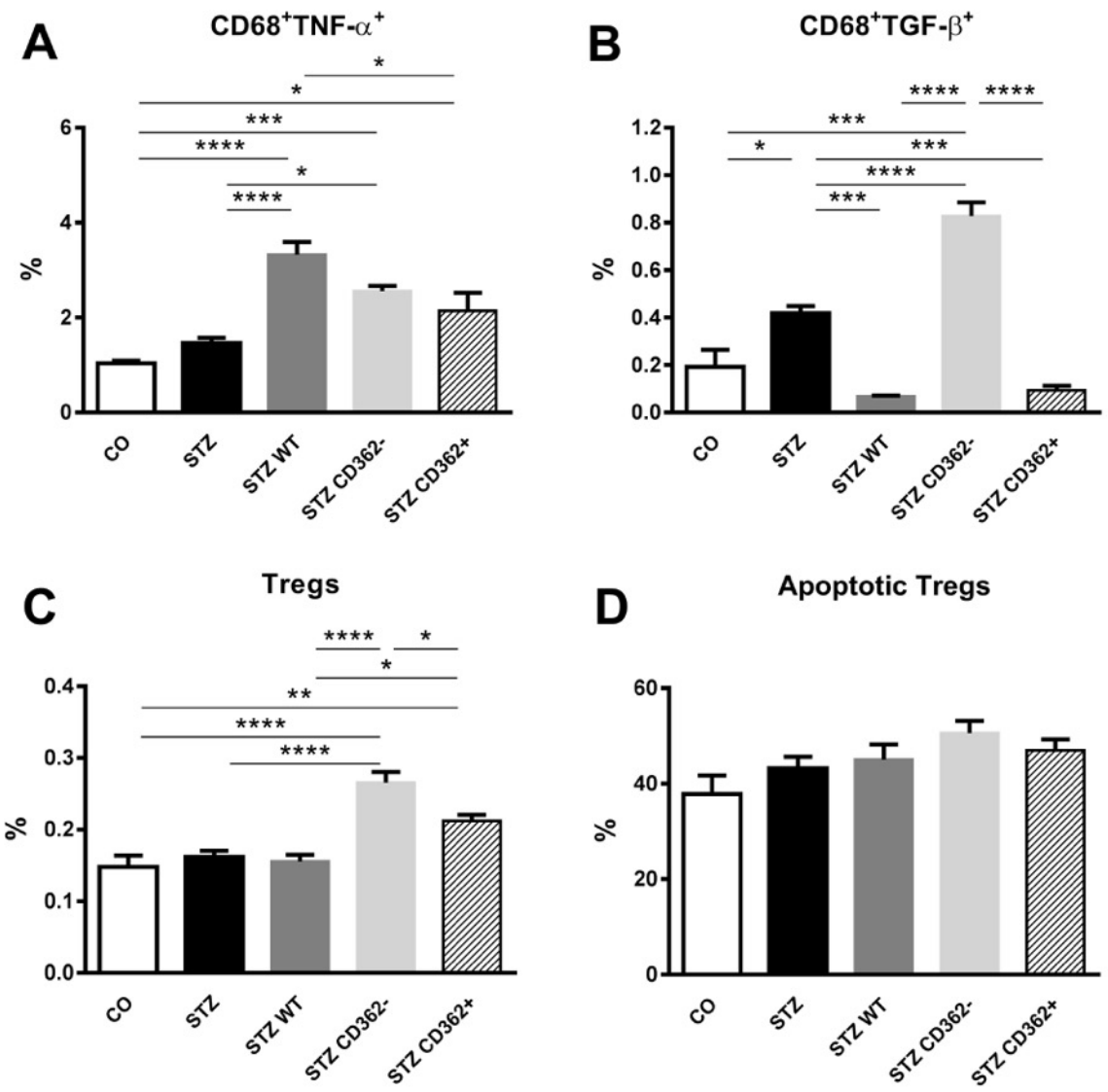

Figure 18. Impact of stromal cells on the immune status of splenocytes isolated from streptozotocin-induced diabetic mice. Bar graphs represent the percentage of **A.** TNF-α-expressing CD68 cells are shown as % of $CD68^+TNF\text{-}\alpha^+$ cells in $CD68^+$ cells, **B.** TGF-ß-expressing CD68 cells are represented as % of $CD68^+TGF\text{-}ß^+$ cells in $CD68^+$ cells, **C.** Tregs shown as % of $CD4^+CD25^+FOXP3^+$ in $CD4^+$ cells and **D.** Apoptotic Tregs represented as % of $CD4^+CD25^+FOXP3^+Annexin\ V^+$ in $CD4^+CD25^+FOXP3^+$ cells, in CO (n=5), STZ (n=5), STZ WT (n=5), STZ $CD362^-$ (n=5) and STZ $CD362^+$ (n=5) groups. Data are expressed as mean ± SEM, p value from One-way-ANOVA. *p<0.05, **p<0.01, ***p<0.001, ****p<0.0001. **Abbreviations:** ANOVA= analysis of variance, apoptotic Tregs= annexin V+ CD4CD25FoxP3+ cells, STZ= streptozotocin, WT= wild type. TGF= transforming growth factor, Tregs= Foxp3-expressing $CD4^+$ $CD25^+$ cells.

4.6 The pro-fibrotic potential of splenocytes

To assess the impact of MSCs application on the pro-fibrotic potential of splenocytes in STZ-induced diabetic mice, splenocytes from each experimental group were co-cultured with fibroblasts for one day and their impact on collagen production of fibroblasts via Sirius red staining was analyzed.

Collagen production in monoculture fibroblasts, and fibroblasts co-cultured with splenocytes isolated from control, STZ, STZ WT, STZ CD362^{-} and STZ CD362^{+} groups was 0.065±0.007,0.065±0.009, 0.092±0.007, 0.092±0.007, 0.090±0.005 and 0.095±0.009, respectively. Collagen production was not significantly different between monocultured fibroblasts and fibroblasts co-cultured with splenocytes derived from control mice, whereas supplementation of splenocytes from STZ mice and STZ CD362^{+} mice led to a 1.5-fold ($p<0.05$) and 1.5-fold ($p<0.05$) higher collagen production compared to monocultured fibroblasts, respectively (**Figure 19**).

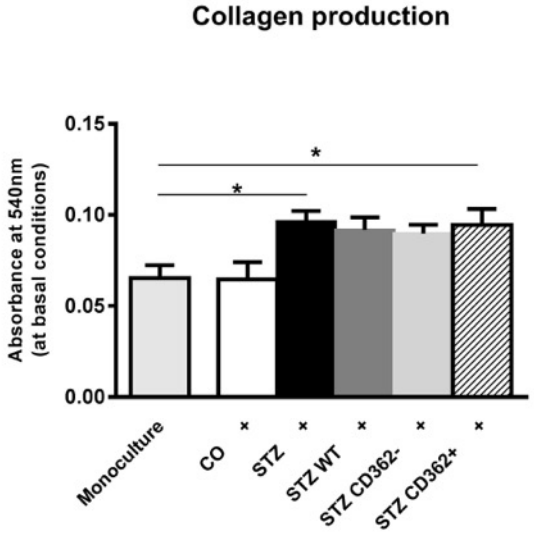

Figure 19. Impact of stromal cells on the pro-fibrotic capacity of splenocytes isolated from streptozotocin-induced diabetic mice. Bar graphs represent the absorbance at 540 nm representing collagen production in monocultured murine fibroblasts (n=10) and fibroblasts co-cultured with splenocytes isolated from CO (n=5), STZ (n=5), STZ WT (n=6), STZ CD362^{-} (n=6) and STZ CD362^{+} (n=6) groups, respectively. Data are expressed as mean ± SEM, p value from One-way-ANOVA. *p<0.05. **Abbreviations:** ANOVA= analysis of variance, CO= control, STZ= streptozotocin, WT= wild type.

5. DISCUSSION

5.1 Main findings

In this experiment, the main findings are as follows: BM-MSCs
do not normalize BG and HbA1c levels in STZ-induced diabetic mice,
do not affect cardiac fibrosis in STZ-induced diabetic mice,
do not affect LV cardiac function in STZ-induced diabetic mice,
regulate immune cell infiltration and splenic immune cell activities in STZ-induced diabetic mice.

5.2 Impact of BM-MSCs on blood glucose and HbA1c in streptozotocin-induced diabetic mice

In vivo studies and clinical trials have demonstrated that MSCs are capable of reducing BG levels in animal models [90-93] and in humans with type 1 DM [94, 95] or type 2 DM [96-98]. Studies [92, 99] have shown that BM-MSCs can increase β cell proliferation and therefore decrease the BG level. It has also been reported that betatrophin overexpressing human adipose-derived MSCs could increase β cell proliferation and ameliorate hyperglycemia and weight loss [93]. Either in patients with type 2 or type 1 DM, MSCs have been demonstrated to decrease BG and increase insulin level by which their protective efficacy depended on the dose used [100]. It is believed that the regenerative and paracrine factors [99] from MSCs play an important role in β cell regeneration and BG normalization by transforming the damaged ß cells to insulin-producing glucose-responsive islet-like clusters in an extract of regenerative factors [101], inhibiting proliferation of pancreatic β-cell-specific T cells and then halting autoimmune destruction of the pancreas and stimulating the regeneration of damaged pancreatic β cells in type 1 DM [102]. In contrast, disappointingly, in this experiment (and in experiments of the other partners of the REDDSTAR consortium), we did not observe BG or HbA1c normalization after BM-MSCs application. This observation is consistent with our own recent findings of i.v. placenta-derived MSC injected in STZ mice, which also did not affect BG levels either [103]. A possible explanation for this discrepancy could be that, in this experiment, allogeneic human BM-MSCs were injected into immunocompetent mice. Whereas MSCs have low immunogenicity, allogeneic MSCs can still be recognized and removed by the receptor's immune system

[102]. In fact, in studies where MSC decreased BG levels, human MSC were injected in severe combined immunodeficient mice [104] or murine MSC were injected in diabetic mice [105]. Another possible reason is that hyperglycemia or sustained high BG levels could affect the cellular metabolism of MSCs, thereby impeding cellular homeostasis which eventually induces senescence, apoptosis and ultimately cell death and finally affects the regenerative ability [106-109]. Especially in this experiment, mice with DM induced by STZ did not receive any other traditional anti-diabetic treatment except for MSCs injection.

5.3 Impact of BM-MSCs on cardiac function in streptozotocin-induced diabetic mice

Studies [110-114] have demonstrated that application of MSCs and other stem cells can improve the cardiac dysfunction in experimental diabetic cardiomyopathy. A recent study further showed that i.v. MSC application can improve diastolic performance in an STZ-induced diabetic cardiomyopathy model with low-grade inflammation, no overt cardiac fibrosis, and with cardiomyocyte stiffness [103]. In the actual STZ model with low-grade inflammation and no cardiac fibrosis, parameters of LV function were not impaired [103, 115]. In contrast, LV function parameters were compensationally increased. One explanation is that the relatively short duration of this experiment was not enough to observe apparent deterioration or amelioration of cardiac function, especially when the pathological process of HF was at an early stage with an adequate contractile reserve. This hypothesis is supported by findings in STZ-induced diabetes in CD1 mice found a gender difference in gender specific progression of diabetic cardiomyopathy. The onset of cardiac dysfunction was more rapid and severe in diabetic females (onset of cardiac diastolic and systolic dysfunction: 8 and 12 weeks after STZ injection, respectively) compared to males (onset of cardiac diastolic and systolic dysfunction: 12 and 20 weeks after STZ injection, respectively) [116]. In STZ-induced diabetic mice [117], mitochondrial impairment has been detected in the absence of cardiac hypertrophy and of resting cardiac performance changes. Therefore, a further possible explanation could be that the cardiac function of the STZ mice could be maintained in a compensatory range with normal or increased hemodynamic parameters. Similarly, an increased EF, and dP/dt_{max} was also found in 12-week old diabetic db/db C57BL/J versus control C57BL/J mice [118]. It has been reported that hemodynamic stress in the form of

adrenalin application could unmask the HF phenotype in $Mlp^{W4R/+}$ and $Mlp^{W4R/W4R}$ knock-in animals, in which the ventricular performance is maintained at the expense of limited myocardial contractile reserve under baseline conditions [119]. In other animal models too, it has been demonstrated that a decline in LV diastolic function could be induced by isoproterenol [117, 120] administration, which leads to positive inotropic and lusitropic effects, like an increase in the contraction force and in the myocardium relaxation rate, respectively, similar to a cardiac work overload.

Neither of the BM-MSCs affected LV function in the STZ mice. To evaluate a potential impact of BM-MSCs in this STZ model with early LV dysfunction, STZ mice should be stressed with isoproterenol or an α1-adrenergic receptor agonist like methoxamine.

5.4 Impact of BM-MSCs on cardiac fibrosis in streptozotocin-induced diabetic mice

Cardiac fibrosis is a characteristic of diabetic cardiomyopathy in type 1 DM [121-123]. Cardiac fibroblasts are responsible for remodeling and fibrosis after injury [124]. Hereby, a population of fibroblasts activated by cytokine and neurohumoral factors, often associated with inflammatory cell accumulation and cardiomyocyte death, rapidly proliferates and becomes activated to express α−SMA and collagen. A central cytokine involved in fibroblast activation is TGF-β [125]. MSCs are known to reduce cardiac fibrosis [110-112, 126] by attenuating the survival, differentiation, proliferation, and collagen synthesis of cardiac fibroblasts [46] as well as by decreasing the profibrotic potential of immune cells [103, 127]. At this stage of STZ-induced DM, cardiac fibrosis was not pronounced, as shown by no induction in LV collagen I, III, and α-SMA expression compared to control mice. Only LV mRNA expression of pro-fibrotic TGF-β was increased versus control mice. Neither of the different BM-MSCs decreased LV TGF-ß mRNA expression or other fibrosis markers.

5.5 Impact of BM-MSCs on immune cell infiltration and splenic immune cell activities in streptozotocin-induced diabetic mice

In parallel to the absence of cardiac fibrosis, this STZ model is associated with low-grade inflammation, i.e. no pronounced inflammatory activation, typically associated with diabetes, obesity, aging, and other chronic inflammatory conditions [128]. This follows from the findings that neither LV mRNA expression of the cytokines TNF-α and

IL-1ß, not of the adhesion molecule VCAM-1 is upregulated, nor is the cardiac presence of $CD68^+$ monocytes/macrophages, $CD4^+$ and $CD8^+$ cells increased. On the other hand, LV expression of the alarmin S100A9, ICAM-1, and the profibrotic factor TGF-ß, was upregulated in STZ compared to control mice. Furthermore, the percentage of splenic CD68 cells expressing TGF-ß was higher in STZ versus control mice, which was further reflected in the higher pro-fibrotic potential of the splenocytes from STZ compared to control mice. The latter observation is in agreement with Van Linthout *et al.* who demonstrated that splenocytes derived from STZ mice increased collagen deposition upon co-culture with fibroblasts compared to fibroblasts in monoculture [103]. This finding corroborates the crosstalk between immune cells and fibrosis [115] and the relevance of the cardiosplenic axis, i.e. the homing of immune cells towards the heart and their subsequent involvement in cardiac remodeling [129]**.** $CD362^+$ and WT-MSCs decreased the STZ-induced percentage of CD68-expressing TGF-ß cells. However, this was not translated into a reduction of profibrotic potential of splenocytes, indicating that cells other than TGF-ß-expressing CD68 cells have a profibrotic potential, which have not been affected by $CD362^+$ and WT-MSCs administration. Conform to the existence of a cardiosplenic axis and in agreement with the unaltered presence of CD68, CD4 and CD8 cells in the heart of STZ versus control mice, cardiac fibrosis was not yet pronounced at this stage of STZ-induced DM mice. In line with the finding that monocytes are a main cellular source of inflammatory cytokines (such as TNF-α, IL-1β) and monocytes were not increased in STZ versus control mice, LV TNF-α and IL-1β expression was not increased in STZ versus control mice. Both cytokines are known to play an important role in diabetic cardiomyopathy [130] and treatment with an interleukin-converting enzyme inhibitor could protect against myocardial inflammation under DM [131].

Expression of the pro-inflammatory adhesion molecules ICAM-1 and VCAM-1 on endothelial cells promotes leukocyte migration by direct binding to leukocyte cell surface receptors, firm adhesion and guidance of monocyte homing into the inflamed tissue [132]. The inflammatory response is dependent on the activation of adhesive interactions between endothelial cells and leukocytes. Persistently high levels of ICAM-1 and VCAM-1 are required for adhesion of leukocytes to the cardiac tissue and for orchestrating the various phases of heart repair. LV ICAM-1 mRNA expression, but not VCAM-1 mRNA expression was increased in STZ versus control mice. The

unchanged LV expression of VCAM-1 in STZ compared to control mice may underlie the unchanged presence of CD68, CD4 and CD8 cells in the LV of STZ versus control mice.

The innate immunity member S100A8/S100A9 is involved in pro-inflammatory processes. This alarmin is abundantly expressed in neutrophils and monocytes and released from damaged and dying cells. This damage DAMP predominantly exists as a heterodimer S100A8/S100A9 and is a ligand of the pattern-recognition receptors, receptor for advanced glycation end products and toll like receptor 4 [133]. As in neutrophils, S100A8/A9 has both extracellular and intracellular effects in monocytes/ macrophages, and extracellular S100A8/A9 enhances the inflammatory cytokine production by human monocytes [134]. In mice with MI, S100A8/S100A9 is rapidly expressed and released after ischemia, primarily by inflammatory cells and fibroblasts, and induces leukocyte infiltration and cardiac dysfunction [135]. In our STZ model, LV S100A9 mRNA was significantly increased compared to control mice, whereas LV S100A8 was only minimally upregulated. This regulation might explain why downstream cytokine expression and the infiltration of monocytes was not yet pronounced at this stage of DM. Nevertheless, it indicates an initiated low-grade inflammatory response.

The immunomodulatory properties of MSCs have been well-documented in DM. MSCs can inhibit T cell proliferation in autologous and allogeneic lymphocyte reactions and increase anti-inflammatory factors [136, 137], reduce the cytotoxicity of cytotoxic T lymphocytes [138] and enhance regulatory T cell (Tregs) proliferation, which can secrete IL-10 and TGF-β [138] and increase the number of Treg [139]. In line with these well-established immunomodulatory properties, $CD362^-$ BM-MSCs raised the % of Tregs, whereas none of the BM-MSCs reduced the number of apoptotic Tregs.

6. PERSPECTIVES

To our knowledge, this is the first study evaluating the potential of CD362-selected BM-MSCs on experimental STZ-induced diabetic cardiomyopathy. This experiment was an unsuccessful attempt to understand the potential benefits of MSC application and particularly of CD362-selected BM-MSCs to treat STZ-induced diabetic cardiomyopathy. There are several limitations, which should be addressed. First, the administration route of MSCs such as intramyocardial injection could be optimized, avoiding the “pulmonary first pass effect” by i.v. injection. Second, methods to improve the viability and homing abilities of MSCs in an hyperglycemic microenvironment should be further considered. Third, in this DM model with no profound cardiac fibrosis, the stiffness of cardiomyocytes and the impact of BM-MSC administration on cardiomyocyte stiffness should be evaluated. Fourth, in this STZ model with early LV dysfunction, the impact of BM-MSC administration on cardiac function under stress conditions needs to be investigated.

BIBLIOGRAPHY

1. Disease GBD, Injury I, Prevalence C: Global, regional, and national incidence, prevalence, and years lived with disability for 310 diseases and injuries, 1990-2015: a systematic analysis for the Global Burden of Disease Study 2015. Lancet 2016, 388(10053):1545-1602.
2. Patterson CC, Dahlquist GG, Gyurus E, Green A, Soltesz G, Group ES: Incidence trends for childhood type 1 diabetes in Europe during 1989-2003 and predicted new cases 2005-20: a multicentre prospective registration study. Lancet 2009, 373(9680):2027-2033.
3. Gaede P, Vedel P, Larsen N, Jensen GV, Parving HH, Pedersen O: Multifactorial intervention and cardiovascular disease in patients with type 2 diabetes. The New England journal of medicine 2003, 348(5):383-393.
4. Tancredi M, Rosengren A, Svensson AM, Kosiborod M, Pivodic A, Gudbjornsdottir S, Wedel H, Clements M, Dahlqvist S, Lind M: Excess Mortality among Persons with Type 2 Diabetes. The New England journal of medicine 2015, 373(18): 1720-1732.
5. Emerging Risk Factors C, Sarwar N, Gao P, Seshasai SR, Gobin R, Kaptoge S, Di Angelantonio E, Ingelsson E, Lawlor DA, Selvin E, Stampfer M, Stehouwer CD, Lewington S, Pennells L, Thompson A, Sattar N, White IR, Ray KK, Danesh J: Diabetes mellitus, fasting blood glucose concentration, and risk of vascular disease: a collaborative meta-analysis of 102 prospective studies. Lancet 2010, 375(9733): 2215-2222.
6. Rubler S, Dlugash J, Yuceoglu YZ, Kumral T, Branwood AW, Grishman A: New type of cardiomyopathy associated with diabetic glomerulosclerosis. The American journal of cardiology 1972, 30(6):595-602.
7. Sarma S, Mentz RJ, Kwasny MJ, Fought AJ, Huffman M, Subacius H, Nodari S, Konstam M, Swedberg K, Maggioni AP, Zannad F, Bonow RO, Gheorghiade M; EVEREST investigators: Association between diabetes mellitus and post-discharge outcomes in patients hospitalized with heart failure: findings from the EVEREST trial. European journal of heart failure 2013, 15(2):194-202.
8. Nichols GA, Gullion CM, Koro CE, Ephross SA, Brown JB: The incidence of congestive heart failure in type 2 diabetes: an update. Diabetes care 2004, 27(8): 1879-1884.

9. Bodiga VL, Eda SR, Bodiga S: Advanced glycation end products: role in pathology of diabetic cardiomyopathy. Heart failure reviews 2014, 19(1):49-63.
10. Linthout SV, Spillmann F, Schultheiss HP, Tschope C: Effects of mesenchymal stromal cells on diabetic cardiomyopathy. Current pharmaceutical design 2011, 17(30): 3341-3347.
11. Rutter MK, Parise H, Benjamin EJ, Levy D, Larson MG, Meigs JB, Nesto RW, Wilson PW, Vasan RS: Impact of glucose intolerance and insulin resistance on cardiac structure and function: sex-related differences in the Framingham Heart Study. Circulation 2003, 107(3):448-454.
12. Devereux RB, Roman MJ, Paranicas M, O'Grady MJ, Lee ET, Welty TK, Fabsitz RR, Robbins D, Rhoades ER, Howard BV: Impact of diabetes on cardiac structure and function: the strong heart study. Circulation 2000, 101(19):2271-2276.
13. Huisamen B, van Zyl M, Keyser A, Lochner A: The effects of insulin and beta-adrenergic stimulation on glucose transport, glut 4 and PKB activation in the myocardium of lean and obese non-insulin dependent diabetes mellitus rats. Molecular and cellular biochemistry 2001, 223(1-2):15-25.
14. Palmieri V, Capaldo B, Russo C, Iaccarino M, Pezzullo S, Quintavalle G, Di Minno G, Riccardi G, Celentano A: Uncomplicated type 1 diabetes and preclinical left ventricular myocardial dysfunction: insights from echocardiography and exercise cardiac performance evaluation. Diabetes research and clinical practice 2008, 79(2):262-268.
15. Russo I, Frangogiannis NG: Diabetes-associated cardiac fibrosis: Cellular effectors, molecular mechanisms and therapeutic opportunities. Journal of molecular and cellular cardiology 2016, 90:84-93.
16. van Hoeven KH, Factor SM: A comparison of the pathological spectrum of hypertensive, diabetic, and hypertensive-diabetic heart disease. Circulation 1990, 82(3): 848-855.
17. Zile MR, Baicu CF, Gaasch WH: Diastolic heart failure--abnormalities in active relaxation and passive stiffness of the left ventricle. The New England journal of medicine 2004, 350(19):1953-1959.
18. Paulus WJ, Tschope C, Sanderson JE, Rusconi C, Flachskampf FA, Rademakers FE, Marino P, Smiseth OA, De Keulenaer G, Leite-Moreira AF, Borbély A, Edes I, Handoko ML, Heymans S, Pezzali N, Pieske B, Dickstein K, Fraser AG, Brutsaert DL: How to diagnose diastolic heart failure: a consensus statement on the

diagnosis of heart failure with normal left ventricular ejection fraction by the Heart Failure and Echocardiography Associations of the European Society of Cardiology. European heart journal 2007, 28(20):2539-2550.

19. Poirier P, Bogaty P, Garneau C, Marois L, Dumesnil JG: Diastolic dysfunction in normotensive men with well-controlled type 2 diabetes: importance of maneuvers in echocardiographic screening for preclinical diabetic cardiomyopathy. Diabetes care 2001, 24(1):5-10.

20. Redfield MM, Jacobsen SJ, Burnett JC, Jr., Mahoney DW, Bailey KR, Rodeheffer RJ: Burden of systolic and diastolic ventricular dysfunction in the community: appreciating the scope of the heart failure epidemic. Jama 2003, 289(2):194-202.

21. von Bibra H, St John Sutton M: Diastolic dysfunction in diabetes and the metabolic syndrome: promising potential for diagnosis and prognosis. Diabetologia 2010, 53(6):1033-1045.

22. Boyer JK, Thanigaraj S, Schechtman KB, Perez JE: Prevalence of ventricular diastolic dysfunction in asymptomatic, normotensive patients with diabetes mellitus. The American journal of cardiology 2004, 93(7):870-875.

23. Shivalkar B, Dhondt D, Goovaerts I, Van Gaal L, Bartunek J, Van Crombrugge P, Vrints C: Flow mediated dilatation and cardiac function in type 1 diabetes mellitus. The American journal of cardiology 2006, 97(1):77-82.

24. Ernande L, Bergerot C, Rietzschel ER, De Buyzere ML, Thibault H, Pignonblanc PG, Croisille P, Ovize M, Groisne L, Moulin P, Gillebert TC, Derumeaux G: Diastolic dysfunction in patients with type 2 diabetes mellitus: is it really the first marker of diabetic cardiomyopathy? Journal of the American Society of Echocardiography : official publication of the American Society of Echocardiography 2011, 24(11):1268-1275 e1261.

25. Boudina S, Abel ED: Diabetic cardiomyopathy revisited. Circulation 2007, 115(25):3213-3223.

26. King AJ: The use of animal models in diabetes research. British journal of pharmacology 2012, 166(3):877-894.

27. Reusser F: Mode of action of streptozotocin. Journal of bacteriology 1971, 105(2):580-588.

28. Goyal SN, Reddy NM, Patil KR, Nakhate KT, Ojha S, Patil CR, Agrawal YO: Challenges and issues with streptozotocin-induced diabetes - A clinically relevant

animal model to understand the diabetes pathogenesis and evaluate therapeutics. Chemico-biological interactions 2016, 244:49-63.

29. Eleazu CO, Eleazu KC, Chukwuma S, Essien UN: Review of the mechanism of cell death resulting from streptozotocin challenge in experimental animals, its practical use and potential risk to humans. Journal of diabetes and metabolic disorders 2013, 12(1):60.

30. Shen X, Bornfeldt KE: Mouse models for studies of cardiovascular complications of type 1 diabetes. Annals of the New York Academy of Sciences 2007, 1103:202-217.

31. Ares-Carrasco S, Picatoste B, Benito-Martin A, Zubiri I, Sanz AB, Sanchez-Nino MD, Ortiz A, Egido J, Tunon J, Lorenzo O: Myocardial fibrosis and apoptosis, but not inflammation, are present in long-term experimental diabetes. American journal of physiology Heart and circulatory physiology 2009, 297(6):H2109-2119.

32. Huynh K, McMullen JR, Julius TL, Tan JW, Love JE, Cemerlang N, Kiriazis H, Du XJ, Ritchie RH: Cardiac-specific IGF-1 receptor transgenic expression protects against cardiac fibrosis and diastolic dysfunction in a mouse model of diabetic cardiomyopathy. Diabetes 2010, 59(6):1512-1520.

33. Nerup J, Mandrup-Poulsen T, Helqvist S, Andersen HU, Pociot F, Reimers JI, Cuartero BG, Karlsen AE, Bjerre U, Lorenzen T: On the pathogenesis of IDDM. Diabetologia 1994, 37 Suppl 2:S82-89.

34. Kim HR, Rho HW, Park BH, Park JW, Kim JS, Kim UH, Chung MY: Role of Ca2+ in alloxan-induced pancreatic beta-cell damage. Biochimica et biophysica acta 1994, 1227(1-2):87-91.

35. Szkudelski T: The mechanism of alloxan and streptozotocin action in B cells of the rat pancreas. Physiological research 2001, 50(6):537-546.

36. Gonzalez-Quesada C, Cavalera M, Biernacka A, Kong P, Lee DW, Saxena A, Frunza O, Dobaczewski M, Shinde A, Frangogiannis NG: Thrombospondin-1 induction in the diabetic myocardium stabilizes the cardiac matrix in addition to promoting vascular rarefaction through angiopoietin-2 upregulation. Circulation research 2013, 113(12):1331-1344.

37. Biernacka A, Cavalera M, Wang J, Russo I, Shinde A, Kong P, Gonzalez-Quesada C, Rai V, Dobaczewski M, Lee DW, Wang XF, Frangogiannis NG: Smad3 Signaling Promotes Fibrosis While Preserving Cardiac and Aortic Geometry in Obese Diabetic Mice. Circulation Heart failure 2015, 8(4):788-798.

38. Lindstrom P: The physiology of obese-hyperglycemic mice [ob/ob mice]. TheScientificWorldJournal 2007, 7:666-685.
39. Standards of Medical Care in Diabetes-2016: Summary of Revisions. Diabetes care 2016, 39 Suppl 1:S4-5.
40. Ponikowski P, Voors AA, Anker SD, Bueno H, Cleland JG, Coats AJ, Falk V, Gonzalez-Juanatey JR, Harjola VP, Jankowska EA, Jessup M, Linde C, Nihoyannopoulos P, Parissis JT, Pieske B, Riley JP, Rosano GMC, Ruilope LM, Ruschitzka F, Rutten FH, van der Meer P; ESC Scientific Document Group: 2016 ESC Guidelines for the diagnosis and treatment of acute and chronic heart failure: The Task Force for the diagnosis and treatment of acute and chronic heart failure of the European Society of Cardiology (ESC)Developed with the special contribution of the Heart Failure Association (HFA) of the ESC. European heart journal 2016, 37(27):2129-2200.
41. Sanganalmath SK, Bolli R: Cell therapy for heart failure: a comprehensive overview of experimental and clinical studies, current challenges, and future directions. Circulation research 2013, 113(6):810-834.
42. Fuchs E, Segre JA: Stem cells: a new lease on life. Cell 2000, 100(1):143-155.
43. Drawnel FM, Boccardo S, Prummer M, Delobel F, Graff A, Weber M, Gerard R, Badi L, Kam-Thong T, Bu L, Jiang X, Hoflack JC, Kiialainen A, Jeworutzki E, Aoyama N, Carlson C, Burcin M, Gromo G, Boehringer M, Stahlberg H, Hall BJ, Magnone MC, Kolaja K, Chien KR, Bailly J, Iacone R: Disease modeling and phenotypic drug screening for diabetic cardiomyopathy using human induced pluripotent stem cells. Cell reports 2014, 9(3):810-821.
44. Cheraghi M, Namdari M, Negahdari B, Eatemadi A: Recent advances in cardiac regeneration: Stem cell, biomaterial and growth factors. Biomedicine & pharmacotherapy = Biomedecine & pharmacotherapie 2017, 87:37-45.
45. Tse HF, Siu CW, Zhu SG, Songyan L, Zhang QY, Lai WH, Kwong YL, Nicholls J, Lau CP: Paracrine effects of direct intramyocardial implantation of bone marrow derived cells to enhance neovascularization in chronic ischaemic myocardium. European journal of heart failure 2007, 9(8):747-753.
46. Mias C, Lairez O, Trouche E, Roncalli J, Calise D, Seguelas MH, Ordener C, Piercecchi-Marti MD, Auge N, Salvayre AN, Bourin P, Parini A, Cussac D: Mesenchymal stem cells promote matrix metalloproteinase secretion by cardiac fibroblasts and reduce

cardiac ventricular fibrosis after myocardial infarction. Stem cells 2009, 27(11): 2734-2743.

47. Friedenstein AJ, Petrakova KV, Kurolesova AI, Frolova GP: Heterotopic of bone marrow. Analysis of precursor cells for osteogenic and hematopoietic tissues. Transplantation 1968, 6(2):230-247.

48. Pittenger MF, Mackay AM, Beck SC, Jaiswal RK, Douglas R, Mosca JD, Moorman MA, Simonetti DW, Craig S, Marshak DR: Multilineage potential of adult human mesenchymal stem cells. Science 1999, 284(5411):143-147.

49. Dominici M, Le Blanc K, Mueller I, Slaper-Cortenbach I, Marini F, Krause D, Deans R, Keating A, Prockop D, Horwitz E: Minimal criteria for defining multipotent mesenchymal stromal cells. The International Society for Cellular Therapy position statement. Cytotherapy 2006, 8(4):315-317.

50. Gronthos S, Graves SE, Ohta S, Simmons PJ: The STRO-1+ fraction of adult human bone marrow contains the osteogenic precursors. Blood 1994, 84(12): 4164-4173.

51. Kuci Z, Seiberth J, Latifi-Pupovci H, Wehner S, Stein S, Grez M, Bonig H, Kohl U, Klingebiel T, Bader P, Kuçi S: Clonal analysis of multipotent stromal cells derived from CD271+ bone marrow mononuclear cells: functional heterogeneity and different mechanisms of allosuppression. Haematologica 2013, 98(10):1609-1616.

52. Sorrentino A, Ferracin M, Castelli G, Biffoni M, Tomaselli G, Baiocchi M, Fatica A, Negrini M, Peschle C, Valtieri M: Isolation and characterization of CD146+ multipotent mesenchymal stromal cells. Experimental hematology 2008, 36(8):1035-1046.

53. Duff SE, Li C, Garland JM, Kumar S: CD105 is important for angiogenesis: evidence and potential applications. FASEB journal: official publication of the Federation of American Societies for Experimental Biology 2003, 17(9):984-992.

54. Alon R, Kassner PD, Carr MW, Finger EB, Hemler ME, Springer TA: The integrin VLA-4 supports tethering and rolling in flow on VCAM-1. The Journal of cell biology 1995, 128(6):1243-1253.

55. Shih IM: The role of CD146 (Mel-CAM) in biology and pathology. The Journal of pathology 1999, 189(1):4-11.

56. Samsonraj RM, Rai B, Sathiyanathan P, Puan KJ, Rotzschke O, Hui JH, Raghunath M, Stanton LW, Nurcombe V, Cool SM: Establishing criteria for human mesenchymal stem cell potency. Stem cells 2015, 33(6):1878-1891.

57. Crisan M, Yap S, Casteilla L, Chen CW, Corselli M, Park TS, Andriolo G, Sun B, Zheng B, Zhang L, Norotte C, Teng PN, Traas J, Schugar R, Deasy BM, Badylak S, Buhring HJ, Giacobino JP, Lazzari L, Huard J, Péault B: A perivascular origin for mesenchymal stem cells in multiple human organs. Cell stem cell 2008, 3(3):301-313.
58. Lendahl U, Zimmerman LB, McKay RD: CNS stem cells express a new class of intermediate filament protein. Cell 1990, 60(4):585-595.
59. Ip JE, Wu Y, Huang J, Zhang L, Pratt RE, Dzau VJ: Mesenchymal stem cells use integrin beta1 not CXC chemokine receptor 4 for myocardial migration and engraftment. Molecular biology of the cell 2007, 18(8):2873-2882.
60. Gao J, Dennis JE, Muzic RF, Lundberg M, Caplan AI: The dynamic in vivo distribution of bone marrow-derived mesenchymal stem cells after infusion. Cells, tissues, organs 2001, 169(1):12-20.
61. Kraitchman DL, Tatsumi M, Gilson WD, Ishimori T, Kedziorek D, Walczak P, Segars WP, Chen HH, Fritzges D, Izbudak I, Young RG, Marcelino M, Pittenger MF, Solaiyappan M, Boston RC, Tsui BM, Wahl RL, Bulte JW: Dynamic imaging of allogeneic mesenchymal stem cells trafficking to myocardial infarction. Circulation 2005, 112(10):1451-1461.
62. Deak E, Seifried E, Henschler R: Homing pathways of mesenchymal stromal cells (MSCs) and their role in clinical applications. International reviews of immunology 2010, 29(5):514-529.
63. Kang SK, Shin IS, Ko MS, Jo JY, Ra JC: Journey of mesenchymal stem cells for homing: strategies to enhance efficacy and safety of stem cell therapy. Stem cells international 2012, 2012:342968.
64. Ryan JM, Barry FP, Murphy JM, Mahon BP: Mesenchymal stem cells avoid allogeneic rejection. Journal of inflammation 2005, 2:8.
65. Le Blanc K, Tammik C, Rosendahl K, Zetterberg E, Ringden O: HLA expression and immunologic properties of differentiated and undifferentiated mesenchymal stem cells. Experimental hematology 2003, 31(10):890-896.
66. Hematti P, Kim J, Stein AP, Kaufman D: Potential role of mesenchymal stromal cells in pancreatic islet transplantation. Transplantation reviews 2013, 27(1):21-29.
67. Quevedo HC, Hatzistergos KE, Oskouei BN, Feigenbaum GS, Rodriguez JE, Valdes D, Pattany PM, Zambrano JP, Hu Q, McNiece I, Heldman AW, Hare JM: Allogeneic mesenchymal stem cells restore cardiac function in chronic ischemic

cardiomyopathy via trilineage differentiating capacity. Proceedings of the National Academy of Sciences of the United States of America 2009, 106(33):14022-14027.

68. Kawada H, Fujita J, Kinjo K, Matsuzaki Y, Tsuma M, Miyatake H, Muguruma Y, Tsuboi K, Itabashi Y, Ikeda Y, Ogawa S, Okano H, Hotta T, Ando K, Fukuda K: Nonhematopoietic mesenchymal stem cells can be mobilized and differentiate into cardiomyocytes after myocardial infarction. Blood 2004, 104(12):3581-3587.

69. Gopinath S, Vanamala SK, Gondi CS, Rao JS: Human umbilical cord blood derived stem cells repair doxorubicin-induced pathological cardiac hypertrophy in mice. Biochemical and biophysical research communications 2010, 395(3):367-372.

70. Ankrum J, Karp JM: Mesenchymal stem cell therapy: Two steps forward, one step back. Trends in molecular medicine 2010, 16(5):203-209.

71. Samper E, Diez-Juan A, Montero JA, Sepulveda P: Cardiac cell therapy: boosting mesenchymal stem cells effects. Stem cell reviews 2013, 9(3):266-280.

72. van den Akker F, de Jager SC, Sluijter JP: Mesenchymal stem cell therapy for cardiac inflammation: immunomodulatory properties and the influence of toll-like receptors. Mediators of inflammation 2013, 2013:181020.

73. Liu H, McTaggart SJ, Johnson DW, Gobe GC: Original article anti-oxidant pathways are stimulated by mesenchymal stromal cells in renal repair after ischemic injury. Cytotherapy 2012, 14(2):162-172.

74. Hatzistergos KE, Quevedo H, Oskouei BN, Hu Q, Feigenbaum GS, Margitich IS, Mazhari R, Boyle AJ, Zambrano JP, Rodriguez JE, Dulce R, Pattany PM, Valdes D, Revilla C, Heldman AW, McNiece I, Hare JM: Bone marrow mesenchymal stem cells stimulate cardiac stem cell proliferation and differentiation. Circulation research 2010, 107(7):913-922.

75. Sarrazin S, Lamanna WC, Esko JD: Heparan sulfate proteoglycans. Cold Spring Harbor perspectives in biology 2011, 3(7).

76. Chen E, Hermanson S, Ekker SC: Syndecan-2 is essential for angiogenic sprouting during zebrafish development. Blood 2004, 103(5):1710-1719.

77. David G, Bai XM, Van der Schueren B, Marynen P, Cassiman JJ, Van den Berghe H: Spatial and temporal changes in the expression of fibroglycan (syndecan-2) during mouse embryonic development. Development 1993, 119(3):841-854.

78. Essner JJ, Chen E, Ekker SC: Syndecan-2. The international journal of biochemistry & cell biology 2006, 38(2):152-156.

79. De Rossi G, Evans AR, Kay E, Woodfin A, McKay TR, Nourshargh S, Whiteford JR: Shed syndecan-2 inhibits angiogenesis. Journal of cell science 2014, 127(Pt 21): 4788-4799.
80. Schellings MW, Vanhoutte D, van Almen GC, Swinnen M, Leenders JJ, Kubben N, van Leeuwen RE, Hofstra L, Heymans S, Pinto YM: Syndecan-1 amplifies angiotensin II-induced cardiac fibrosis. Hypertension 2010, 55(2):249-256.
81. Vanhoutte D, Schellings MW, Gotte M, Swinnen M, Herias V, Wild MK, Vestweber D, Chorianopoulos E, Cortes V, Rigotti A, Stepp MA, Van de Werf F, Carmeliet P, Pinto YM, Heymans S: Increased expression of syndecan-1 protects against cardiac dilatation and dysfunction after myocardial infarction. Circulation 2007, 115(4):475-482.
82. Li G, Xie J, Chen J, Li R, Wu H, Zhang X, Chen Q, Gu R, Xu B: Syndecan-4 deficiency accelerates the transition from compensated hypertrophy to heart failure following pressure overload. Cardiovascular pathology : the official journal of the Society for Cardiovascular Pathology 2017, 28:74-79.
83. Strunz CM, Matsuda M, Salemi VM, Nogueira A, Mansur AP, Cestari IN, Marquezini MV: Changes in cardiac heparan sulfate proteoglycan expression and streptozotocin-induced diastolic dysfunction in rats. Cardiovascular diabetology 2011, 10:35.
84. Rajesh M, Mukhopadhyay P, Batkai S, Patel V, Saito K, Matsumoto S, Kashiwaya Y, Horvath B, Mukhopadhyay B, Becker L, Haskó G, Liaudet L, Wink DA, Veves A, Mechoulam R, Pacher P: Cannabidiol attenuates cardiac dysfunction, oxidative stress, fibrosis, and inflammatory and cell death signaling pathways in diabetic cardiomyopathy. Journal of the American College of Cardiology 2010, 56(25):2115-2125.
85. Ritchie RH, Love JE, Huynh K, Bernardo BC, Henstridge DC, Kiriazis H, Tham YK, Sapra G, Qin C, Cemerlang N, Boey EJ, Jandeleit-Dahm K, Du XJ, McMullen JR: Enhanced phosphoinositide 3-kinase(p110alpha) activity prevents diabetes-induced cardiomyopathy and superoxide generation in a mouse model of diabetes. Diabetologia 2012, 55(12):3369-3381.
86. Pacher P, Nagayama T, Mukhopadhyay P, Batkai S, Kass DA: Measurement of cardiac function using pressure-volume conductance catheter technique in mice and rats. Nature protocols 2008, 3(9):1422-1434.

87. Baan J, van der Velde ET, de Bruin HG, Smeenk GJ, Koops J, van Dijk AD, Temmerman D, Senden J, Buis B: Continuous measurement of left ventricular volume in animals and humans by conductance catheter. Circulation 1984, 70(5):812-823.
88. Ramos-Vara JA, Miller MA: When tissue antigens and antibodies get along: revisiting the technical aspects of immunohistochemistry--the red, brown, and blue technique. Veterinary pathology 2014, 51(1):42-87.
89. Radonic A, Thulke S, Mackay IM, Landt O, Siegert W, Nitsche A: Guideline to reference gene selection for quantitative real-time PCR. Biochemical and biophysical research communications 2004, 313(4):856-862.
90. Aali E, Mirzamohammadi S, Ghaznavi H, Madjd Z, Larijani B, Rayegan S, Sharifi AM: A comparative study of mesenchymal stem cell transplantation with its paracrine effect on control of hyperglycemia in type 1 diabetic rats. Journal of diabetes and metabolic disorders 2014, 13(1):76.
91. Bhansali S, Kumar V, Saikia UN, Medhi B, Jha V, Bhansali A, Dutta P: Effect of mesenchymal stem cells transplantation on glycaemic profile & their localization in streptozotocin induced diabetic Wistar rats. The Indian journal of medical research 2015, 142(1):63-71.
92. El Barky AR, Ezz AAH, Alm-Eldeen AA, Hussein SA, Hafez YA, Mohamed TM: Can Stem Cells Ameliorate the Pancreatic Damage Induced by Streptozotocin in Rats? Canadian journal of diabetes 2017.
93. Sun LL, Liu TJ, Li L, Tang W, Zou JJ, Chen XF, Zheng JY, Jiang BG, Shi YQ: Transplantation of betatrophin-expressing adipose-derived mesenchymal stem cells induces beta-cell proliferation in diabetic mice. International journal of molecular medicine 2017, 39(4):936-948.
94. Cai J, Wu Z, Xu X, Liao L, Chen J, Huang L, Wu W, Luo F, Wu C, Pugliese A, Pileggi A, Ricordi C, Tan J: Umbilical Cord Mesenchymal Stromal Cell With Autologous Bone Marrow Cell Transplantation in Established Type 1 Diabetes: A Pilot Randomized Controlled Open-Label Clinical Study to Assess Safety and Impact on Insulin Secretion. Diabetes care 2016, 39(1):149-157.
95. Li L, Hui H, Jia X, Zhang J, Liu Y, Xu Q, Zhu D: Infusion with Human Bone Marrow-derived Mesenchymal Stem Cells Improves beta-cell Function in Patients and Non-obese Mice with Severe Diabetes. Scientific reports 2016, 6:37894.

96. Hu J, Li C, Wang L, Zhang X, Zhang M, Gao H, Yu X, Wang F, Zhao W, Yan S, Wang Y: Long term effects of the implantation of autologous bone marrow mononuclear cells for type 2 diabetes mellitus. Endocrine journal 2012, 59(11):1031-1039.
97. Skyler JS, Fonseca VA, Segal KR, Rosenstock J, Investigators M-D: Allogeneic Mesenchymal Precursor Cells in Type 2 Diabetes: A Randomized, Placebo-Controlled, Dose-Escalation Safety and Tolerability Pilot Study. Diabetes care 2015, 38(9): 1742-1749.
98. Bhansali S, Dutta P, Kumar V, Yadav MK, Jain A, Mudaliar S, Bhansali S, Sharma RR, Jha V, Marwaha N, Khandelwal N, Srinivasan A, Sachdeva N, Hawkins M, Bhansali A: Efficacy of Autologous Bone Marrow-Derived Mesenchymal Stem Cell and Mononuclear Cell Transplantation in Type 2 Diabetes Mellitus: A Randomized, Placebo-Controlled Comparative Study. Stem cells and development 2017, 26(7):471-481.
99. Gao X, Song L, Shen K, Wang H, Qian M, Niu W, Qin X: Bone marrow mesenchymal stem cells promote the repair of islets from diabetic mice through paracrine actions. Molecular and cellular endocrinology 2014, 388(1-2):41-50.
100. Yaochite JN, Caliari-Oliveira C, de Souza LE, Neto LS, Palma PV, Covas DT, Malmegrim KC, Voltarelli JC, Donadi EA: Therapeutic efficacy and biodistribution of allogeneic mesenchymal stem cells delivered by intrasplenic and intrapancreatic routes in streptozotocin-induced diabetic mice. Stem cell research & therapy 2015, 6:31.
101. Carlsson PO, Schwarcz E, Korsgren O, Le Blanc K: Preserved beta-cell function in type 1 diabetes by mesenchymal stromal cells. Diabetes 2015, 64(2):587-592.
102. Fiorina P, Jurewicz M, Augello A, Vergani A, Dada S, La Rosa S, Selig M, Godwin J, Law K, Placidi C, Smith RN, Capella C, Rodig S, Adra CN, Atkinson M, Sayegh MH, Abdi R: Immunomodulatory function of bone marrow-derived mesenchymal stem cells in experimental autoimmune type 1 diabetes. Journal of immunology 2009, 183(2): 993-1004.
103. Van Linthout S, Hamdani N, Miteva K, Koschel A, Muller I, Pinzur L, Aberman Z, Pappritz K, Linke WA, Tschope C: Placenta-Derived Adherent Stromal Cells Improve Diabetes Mellitus-Associated Left Ventricular Diastolic Performance. Stem cells translational medicine 2017, 6(12):2135-2145.
104. Lee RH, Seo MJ, Reger RL, Spees JL, Pulin AA, Olson SD, Prockop DJ: Multipotent stromal cells from human marrow home to and promote repair of pancreatic

islets and renal glomeruli in diabetic NOD/scid mice. Proceedings of the National Academy of Sciences of the United States of America 2006, 103(46):17438-17443.

105. Ezquer FE, Ezquer ME, Parrau DB, Carpio D, Yanez AJ, Conget PA: Systemic administration of multipotent mesenchymal stromal cells reverts hyperglycemia and prevents nephropathy in type 1 diabetic mice. Biology of blood and marrow transplantation : journal of the American Society for Blood and Marrow Transplantation 2008, 14(6):631-640.

106. Stolzing A, Coleman N, Scutt A: Glucose-induced replicative senescence in mesenchymal stem cells. Rejuvenation research 2006, 9(1):31-35.

107. Yokoi T, Fukuo K, Yasuda O, Hotta M, Miyazaki J, Takemura Y, Kawamoto H, Ichijo H, Ogihara T: Apoptosis signal-regulating kinase 1 mediates cellular senescence induced by high glucose in endothelial cells. Diabetes 2006, 55(6):1660-1665.

108. Cramer C, Freisinger E, Jones RK, Slakey DP, Dupin CL, Newsome ER, Alt EU, Izadpanah R: Persistent high glucose concentrations alter the regenerative potential of mesenchymal stem cells. Stem cells and development 2010, 19(12):1875-1884.

109. Molgat AS, Tilokee EL, Rafatian G, Vulesevic B, Ruel M, Milne R, Suuronen EJ, Davis DR: Hyperglycemia inhibits cardiac stem cell-mediated cardiac repair and angiogenic capacity. Circulation 2014, 130(11 Suppl 1):S70-76.

110. Abdel Aziz MT, El-Asmar MF, Haidara M, Atta HM, Roshdy NK, Rashed LA, Sabry D, Youssef MA, Abdel Aziz AT, Moustafa M: Effect of bone marrow-derived mesenchymal stem cells on cardiovascular complications in diabetic rats. Medical science monitor : international medical journal of experimental and clinical research 2008, 14(11):BR249-255.

111. Cheng Y, Guo S, Liu G, Feng Y, Yan B, Yu J, Feng K, Li Z: Transplantation of bone marrow-derived endothelial progenitor cells attenuates myocardial interstitial fibrosis and cardiac dysfunction in streptozotocin-induced diabetic rats. International journal of molecular medicine 2012, 30(4):870-876.

112. Khan M, Ali F, Mohsin S, Akhtar S, Mehmood A, Choudhery MS, Khan SN, Riazuddin S: Preconditioning diabetic mesenchymal stem cells with myogenic medium increases their ability to repair diabetic heart. Stem cell research & therapy 2013, 4(3): 58.

113. Yan B, Singla DK: Transplanted induced pluripotent stem cells mitigate oxidative stress and improve cardiac function through the Akt cell survival pathway in diabetic cardiomyopathy. Molecular pharmaceutics 2013, 10(9):3425-3432.
114. Dong X, Zhu F, Liu Q, Zhang Y, Wu J, Jiang W, Zhang L, Dong S: Transplanted bone marrow mesenchymal stem cells protects myocardium by regulating 14-3-3 protein in a rat model of diabetic cardiomyopathy. International journal of clinical and experimental pathology 2014, 7(7):3714-3723.
115. Van Linthout S, Miteva K, Tschope C: Crosstalk between fibroblasts and inflammatory cells. Cardiovascular research 2014, 102(2):258-269.
116. Moore A, Shindikar A, Fomison-Nurse I, Riu F, Munasinghe PE, Ram TP, Saxena P, Coffey S, Bunton RW, Galvin IF, Williams MJ, Emanueli C, Madeddu P, Katare R1: Rapid onset of cardiomyopathy in STZ-induced female diabetic mice involves the downregulation of pro-survival Pim-1. Cardiovascular diabetology 2014, 13:68.
117. Bombicino SS, Iglesias DE, Mikusic IA, D'Annunzio V, Gelpi RJ, Boveris A, Valdez LB: Diabetes impairs heart mitochondrial function without changes in resting cardiac performance. The international journal of biochemistry & cell biology 2016, 81(Pt B):335-345.
118. van den Berg SM, Seijkens TT, Kusters PJ, Beckers L, den Toom M, Smeets E, Levels J, de Winther MP, Lutgens E: Diet-induced obesity in mice diminishes hematopoietic stem and progenitor cells in the bone marrow. FASEB journal : official publication of the Federation of American Societies for Experimental Biology 2016, 30(5):1779-1788.
119. Knoll R, Kostin S, Klede S, Savvatis K, Klinge L, Stehle I, Gunkel S, Kotter S, Babicz K, Sohns M, Miocic S, Didié M, Knöll G, Zimmermann WH, Thelen P, Bickeböller H, Maier LS, Schaper W, Schaper J, Kraft T, Tschöpe C, Linke WA, Chien KR: A common MLP (muscle LIM protein) variant is associated with cardiomyopathy. Circulation research 2010, 106(4):695-704.
120. Westermann D, Knollmann BC, Steendijk P, Rutschow S, Riad A, Pauschinger M, Potter JD, Schultheiss HP, Tschope C: Diltiazem treatment prevents diastolic heart failure in mice with familial hypertrophic cardiomyopathy. European journal of heart failure 2006, 8(2):115-121.
121. Tschope C, Walther T, Koniger J, Spillmann F, Westermann D, Escher F, Pauschinger M, Pesquero JB, Bader M, Schultheiss HP, Noutsias M: Prevention of

cardiac fibrosis and left ventricular dysfunction in diabetic cardiomyopathy in rats by transgenic expression of the human tissue kallikrein gene. FASEB journal : official publication of the Federation of American Societies for Experimental Biology 2004, 18(7):828-835.

122. Van Linthout S, Riad A, Dhayat N, Spillmann F, Du J, Dhayat S, Westermann D, Hilfiker-Kleiner D, Noutsias M, Laufs U, Schultheiss HP, Tschöpe C: Anti-inflammatory effects of atorvastatin improve left ventricular function in experimental diabetic cardiomyopathy. Diabetologia 2007, 50(9):1977-1986.

123. Van Linthout S, Spillmann F, Riad A, Trimpert C, Lievens J, Meloni M, Escher F, Filenberg E, Demir O, Li J, Shakibaei M, Schimke I, Staudt A, Felix SB, Schultheiss HP, De Geest B, Tschöpe C: Human apolipoprotein A-I gene transfer reduces the development of experimental diabetic cardiomyopathy. Circulation 2008, 117(12): 1563-1573.

124. Tallquist MD, Molkentin JD: Redefining the identity of cardiac fibroblasts. Nature reviews Cardiology 2017, 14(8):484-491.

125. Stempien-Otero A, Kim DH, Davis J: Molecular networks underlying myofibroblast fate and fibrosis. Journal of molecular and cellular cardiology 2016, 97:153-161.

126. Zhang N, Li J, Luo R, Jiang J, Wang JA: Bone marrow mesenchymal stem cells induce angiogenesis and attenuate the remodeling of diabetic cardiomyopathy. Experimental and clinical endocrinology & diabetes : official journal, German Society of Endocrinology [and] German Diabetes Association 2008, 116(2):104-111.

127. Savvatis K, van Linthout S, Miteva K, Pappritz K, Westermann D, Schefold JC, Fusch G, Weithauser A, Rauch U, Becher PM, Klingel K, Ringe J, Kurtz A, Schultheiss HP, Tschöpe C: Mesenchymal stromal cells but not cardiac fibroblasts exert beneficial systemic immunomodulatory effects in experimental myocarditis. PloS one 2012, 7(7):e41047.

128. Van Linthout S, Tschope C: Inflammation - Cause or Consequence of Heart Failure or Both? Current heart failure reports 2017, 14(4):251-265.

129. Ismahil MA, Hamid T, Bansal SS, Patel B, Kingery JR, Prabhu SD: Remodeling of the mononuclear phagocyte network underlies chronic inflammation and disease progression in heart failure: critical importance of the cardiosplenic axis. Circulation research 2014, 114(2):266-282.

130. Westermann D, Van Linthout S, Dhayat S, Dhayat N, Schmidt A, Noutsias M, Song XY, Spillmann F, Riad A, Schultheiss HP, Tschöpe C: Tumor necrosis factor-alpha antagonism protects from myocardial inflammation and fibrosis in experimental diabetic cardiomyopathy. Basic research in cardiology 2007, 102(6):500-507.
131. Westermann D, Van Linthout S, Dhayat S, Dhayat N, Escher F, Bucker-Gartner C, Spillmann F, Noutsias M, Riad A, Schultheiss HP, Tschöpe C: Cardioprotective and anti-inflammatory effects of interleukin converting enzyme inhibition in experimental diabetic cardiomyopathy. Diabetes 2007, 56(7):1834-1841.
132. Ghigo A, Franco I, Morello F, Hirsch E: Myocyte signalling in leucocyte recruitment to the heart. Cardiovascular research 2014, 102(2):270-280.
133. Eggers K, Sikora K, Lorenz M, Taubert T, Moobed M, Baumann G, Stangl K, Stangl V: RAGE-dependent regulation of calcium-binding proteins S100A8 and S100A9 in human THP-1. Experimental and clinical endocrinology & diabetes : official journal, German Society of Endocrinology [and] German Diabetes Association 2011, 119(6): 353-357.
134. Sunahori K, Yamamura M, Yamana J, Takasugi K, Kawashima M, Yamamoto H, Chazin WJ, Nakatani Y, Yui S, Makino H: The S100A8/A9 heterodimer amplifies proinflammatory cytokine production by macrophages via activation of nuclear factor kappa B and p38 mitogen-activated protein kinase in rheumatoid arthritis. Arthritis research & therapy 2006, 8(3):R69.
135. Volz HC, Laohachewin D, Seidel C, Lasitschka F, Keilbach K, Wienbrandt AR, Andrassy J, Bierhaus A, Kaya Z, Katus HA, Andrassy M: S100A8/A9 aggravates post-ischemic heart failure through activation of RAGE-dependent NF-kappaB signaling. Basic research in cardiology 2012, 107(2):250.
136. Le Blanc K, Rasmusson I, Gotherstrom C, Seidel C, Sundberg B, Sundin M, Rosendahl K, Tammik C, Ringden O: Mesenchymal stem cells inhibit the expression of CD25 (interleukin-2 receptor) and CD38 on phytohaemagglutinin-activated lymphocytes. Scandinavian journal of immunology 2004, 60(3):307-315.
137. Bassi EJ, Moraes-Vieira PM, Moreira-Sa CS, Almeida DC, Vieira LM, Cunha CS, Hiyane MI, Basso AS, Pacheco-Silva A, Camara NO: Immune regulatory properties of allogeneic adipose-derived mesenchymal stem cells in the treatment of experimental autoimmune diabetes. Diabetes 2012, 61(10):2534-2545.

138. Luz-Crawford P, Kurte M, Bravo-Alegria J, Contreras R, Nova-Lamperti E, Tejedor G, Noel D, Jorgensen C, Figueroa F, Djouad F, Carrión F: Mesenchymal stem cells generate a CD4+CD25+Foxp3+ regulatory T cell population during the differentiation process of Th1 and Th17 cells. Stem cell research & therapy 2013, 4(3): 65.

139. Maccario R, Podesta M, Moretta A, Cometa A, Comoli P, Montagna D, Daudt L, Ibatici A, Piaggio G, Pozzi S, Frassoni F, Locatelli F: Interaction of human mesenchymal stem cells with cells involved in alloantigen-specific immune response favors the differentiation of CD4+ T-cell subsets expressing a regulatory/suppressive phenotype. Haematologica 2005, 90(4):516-525.

EIDESSTATTLICHE VERSICHERUNG

„Ich, **Gang Huang**, versichere an Eides statt durch meine eigenhändige Unterschrift, dass ich die vorgelegte Dissertation mit dem Thema: **Impact of mesenchymal stromal cells on streptozotocin-induced diabetic cardiomyopathy** selbstständig und ohne nicht offengelegte Hilfe Dritter verfasst und keine anderen als die angegebenen Quellen und Hilfsmittel genutzt habe.
Alle Stellen, die wörtlich oder dem Sinne nach auf Publikationen oder Vorträgen anderer Autoren beruhen, sind als solche in korrekter Zitierung (siehe „Uniform Requirements for Manuscripts (URM)“ des ICMJE -www.icmje.org) kenntlich gemacht. Die Abschnitte zu Methodik (insbesondere praktische Arbeiten, Laborbestimmungen, statistische Aufarbeitung) und Resultaten (insbesondere Abbildungen, Graphiken und Tabellen) entsprechen den URM (s.o) und werden von mir verantwortet.
Meine Anteile an etwaigen Publikationen zu dieser Dissertation entsprechen denen, die in der untenstehenden gemeinsamen Erklärung mit dem/der Betreuer/in, angegeben sind. Sämtliche Publikationen, die aus dieser Dissertation hervorgegangen sind und bei denen ich Autor bin, entsprechen den URM (s.o) und werden von mir verantwortet.

Die Bedeutung dieser eidesstattlichen Versicherung und die strafrechtlichen Folgen einer unwahren eidesstattlichen Versicherung (§156,161 des Strafgesetzbuches) sind mir bekannt und bewusst.“

Datum Unterschrift:

CURRICULUM VITAE

My curriculum vitae does not appear in the electronic version of my paper for reasons of data protection.

PUBLIKATIONSLISTE UND KONGRESSBEITRÄGE

My curriculum vitae does not appear in the electronic version of my paper for reasons of data protection.

ACKNOWLEDGEMENTS

I would like to acknowledge and thank all people who supported and helped me during my unforgettable stay in Berlin.

Firstly, I would like to express my sincere gratitude to my supervisor, Prof. Dr. Carsten Tschöpe, for offering this great opportunity to study in his working group. Especially, I would like to thank my second supervisor, PD Dr. Sophie Van Linthout, for her insightful suggestions, helpful comments, and numerous corrections for the writing of this dissertation. Without her help, completion of this dissertation would not have been possible.

Secondly, I am very grateful to (in alphabetical order) Mr. Fengquan Dong, Ms. Annika Koschel, Mr. Jie Lin, Dr. Irene Müller, Dr. Kapka Miteva, Dr. Kathleen Pappritz, Ms. Kerstin Puhl and Ms. Marzena Sosnowski for their valuable technical assistance and Dr. Irene Müller and Dr. Kathleen Pappritz for their assistance in thesis writing.

Thirdly, to all my friends, I am especially thankful for the help from Mr. Shenghao Zheng and Ms Pamela Glowacki in solving all the difficulties at the beginning of my stay in Berlin.

Finally, but not lastly, my warmest appreciation goes to my family in China, for their love, encouragement, and support.